BRNO UNIVERSITY OF TECHNOLOGY
VYSOKÉ UČENÍ TECHNICKÉ V BRNĚ

FACULTY OF MECHANICAL ENGINEERING
FAKULTA STROJNÍHO INŽENÝRSTVÍ

INSTITUTE OF MATHEMATICS
ÚSTAV MATEMATIKY

THE LORENZ SYSTEM: A ROUTE FROM STABILITY TO CHAOS
LORENZŮV SYSTÉM: CESTA OD STABILITY K CHAOSU

MASTER'S THESIS
DIPLOMOVÁ PRÁCE

AUTHOR — **BSc Daniel Andoh Arhinful**
AUTOR PRÁCE

SUPERVISOR — **doc. Mgr. Pavel Řehák, Ph.D.**
VEDOUCÍ PRÁCE

BRNO 2020

BRNO UNIVERSITY OF TECHNOLOGY
FACULTY OF MECHANICAL ENGINEERING

Specification Master's Thesis

Department:	Institute of Mathematics
Student:	**BSc Daniel Andoh Arhinful**
Study programme:	Applied Sciences in Engineering
Study branch:	Mathematical Engineering
Supervisor:	**doc. Mgr. Pavel Řehák, Ph.D.**
Academic year:	2019/20

Pursuant to Act no. 111/1998 concerning universities and the BUT study and examination rules, you have been assigned the following topic by the institute director Master's Thesis:

The Lorenz system: A route from stability to chaos

Concise characteristic of the task:

The Lorenz system is a typical representative of chaotic systems which are characteristic by their quite complicated behavior and high sensitivity to initial conditions. Its origin goes back to the work of E. Lorenz who attempted to model a convection in the atmosphere, but it can serve as a mathematical description of some other phenomena.

Goals Master's Thesis:

1. A description of how Lorenz equations arise in various models.
2. Understanding of selected concepts from the theory of nonlinear systems (such as equilibrium point, stability, linearization, bifurcation, Lyapunov function, (deterministic) chaos, (strange) attractor, Lyapunov exponent, etc.).
3. Analysis of the routes from stability to chaos and discussion of bifurcation scenarios.
4. Numerical testing of theoretical results and their graphical interpretation.

Recommended bibliography:

HIRSCH, M. W., SMALE, S., DEVANEY, R. Differential Equations, Dynamical Systems & An Introduction to Chaos, Elsevier, 2003.

ROBINSON, R. C. An Introduction to Dynamical Systems — Continuous and Discrete, 2nd ed., American Mathematical Society, Providence, 2012.

STROGATZ, S. H. Nonlinear Dynamics and Chaos, 2nd ed., Westview Press, 2015.

Deadline for submission Master's Thesis is given by the Schedule of the Academic year 2019/20

In Brno,

L. S.

prof. RNDr. Josef Šlapal, CSc. Director of the Institute	doc. Ing. Jaroslav Katolický, Ph.D. FME dean

Abstract

The theory of deterministic chaos has generated a lot of interest and continues to be one of the much-focused research areas in the field of dynamics today. This is due to its prevalence in essential parts of human lives such as electrical circuits, chemical reactions, the flow of blood through the human system, the weather, etc. This thesis presents a study of the Lorenz equations, a famous example of chaotic systems. In particular, it presents the analysis of the Lorenz equations from stability to chaos and various bifurcation scenarios with numerical and graphical interpretations. It studies concepts of non-linear dynamical systems such as equilibrium points, stability, linearization, bifurcation, Lyapunov function, etc. Finally, it discusses how the Lorenz equations serve as a model for the waterwheel (in detail), and the convection roll for fluid.

Keywords

Lorenz equations, Non-linear systems, Equilibrium points, Stability, Linearization, Bifurcation, Lyapunov function, Waterwheel and Convection roll.

ARHINFUL, Daniel Andoh. Lorenz's system: *the route from stability to chaos* [online]. Brno, 2020 [cit. 2020-06-15] . Available from: https://www.vutbr.cz/en/studenti/zav-prace/detail/124446 . Thesis. Brno University of Technology, Faculty of Mechanical Engineering, Department of Mathematics. Thesis supervisor Pavel Řehák.

I declare that I have worked on this thesis independently under the supervision of doc. Mgr. Pavel Řehák, Ph.D and using the sources listed in the bibliography.

BSc Daniel Andoh Arhinful

I would like to thank my supervisor, doc. Mgr. Pavel Řehák, Ph.D. for his time, advice and the materials he provided for this thesis.

Contents

1. Introduction

The word chaos is borrowed from the ancient Greek word "abyss" which meant void. The meaning has metamorphosed through different meanings before getting its current meaning as disorder. Some definitions also define chaos as disarray, disorganization or confusion. Today scientists use chaos to describe complex systems whose behaviour is so unpredictable, random and highly sensitive to small change in condition or perturbation. (Deterministic) chaos does not mean completely messy or disorder as many may think, in fact, chaotic systems are predictable but only for a very short while before entering into duration of chaos. This makes future predictions difficult. Chaos is essential area of dynamics which has been studied since Newton's time when he proposed the concept of Newtonian mechanics. The theory of chaos has generated a lot of interest and continuous to be one of the much focused research areas in the field of dynamics today. This is due to its prevalence in most aspect of human life, such as in the behaviour of the weather, airplanes in flight, flow of oil in underground pipes, flow of blood through the human system, etc. which we cannot ignore. Another reason for the arousing interest in the study of chaos is the fascinating history to its discovery. Before the discovery of chaos in deterministic models, people believed classical mechanics were predictable provided you have the necessary instrument to take measurement or the mathematical skills to solve the system. This is captured in Gleick's book [5] where he quoted one physicist who said "Relativity eliminated the Newtonian illusion of absolute space and time; quantum theory eliminated the Newtonian dream of a controllable measurement process; and chaos eliminates the Laplacian fantasy of deterministic predictability." There are many chaotic systems, however the Lorenz system is popular and perhaps the most studied chaotic system. This is due to the complexity of the system, and also serving as model for other physical and practical phenomena such as the convection roll for fluid, chaotic waterwheel and its application in generating secret messages. For these reasons, we have chosen to study the Lorenz system.

1.1. Thesis Objectives

This research seeks to achieve the following:

1. To study a description of how Lorenz equations arise in various models
2. To study selected concepts from the theory of nonlinear systems (such as equilibrium point, stability, linearization, bifurcation, Lyapunov function, (deterministic) chaos, (strange) attractor, Lyapunov exponent, etc.)
3. To study the routes from stability to chaos and discussion of bifurcation scenarios.
4. Numerical testing of theoretical results and their graphical interpretation.

1.2. Organisation of Work

This research has six chapters. Chapter 1 talks about general introduction to our research. It includes specific objectives of the thesis. Chapter 2 reviews some relevant literature in

the area of study with a brief history of the subject. Chapter 3 explains the methods used and their applications to the study. Chapter 4 discusses the analysis and simulation of the Lorenz system. Chapter 5 talks about some physical models the Lorenz equations model. The final part of the thesis includes conclusion of results and some recommendations.

2. Literature Review

In the early 1600s, physicists focused on exploring the astronomy and the beauty of planetary motions. Specifically, most physicists tried to solve the two-body problem - the problem of calculating the motion of Earth around the Sun given the inverse – square law of attraction between them. The problem remained unsolved after several attempts by physicists and mathematicians. However, in the mid-1600s, the problem saw the light of the day when Newton solved the problem with differential equation he invented and laws of motion he had discovered. Newton tried to extend his discovery to solving three-body problem (the Sun, Earth and Moon) which he formulated in 1687. The solution to the three body was practically necessary to accurately determine marine navigation at sea [9]. After decades of effort, the problem seemed impossible to solve. He admitted that the three body problem was very difficult to solve and this grew the interest of many physicists and mathematicians to the problem.

Henri Poincaré developed qualitative methods to solve differential equations and used them to identify and study possible periodic orbits. Poincaré's new qualitative approach led him to identify the unpredictability of the problem, and to discovery of a new complex phenomenon which is known as chaos [9], [10]. Poincaré had the first glimpse of the complexity, chaos; in which a deterministic model shows nonperiodic behaviour that depends sensitively on the initial conditions, making long-term prediction impossible. In 1887, in honour of his 60th birthday, King Oscar II, king of Sweden established in collaboration with the Acta Mathematica Journal, a competition to award anyone who could solve the three body problem. Poincaré's incredible contributions won him the King's prize [1], [2]. Poincaré's discovery of chaos did not receive much attention in the first half of the twentieth century; instead dynamics was largely concerned with nonlinear oscillator and their applications in physics and engineering [16].

Edward Lorenz is known as the man who reintroduced the theory of chaos when he encountered one himself during his experiment. In 1960, E. N Lorenz working as meteorologist at MIT embarked on a research to simulate and predict the weather. Lorenz came up with twelve variables he believed could predict the weather. They were numerical rules – equations that expressed the relationships between temperature, pressure, and wind speed [5]. Lorenz had developed a deterministic model which he would simulate, yet could not predict the outcome. In an attempt to try a new approach, Lorenz decided to take a shortcut. He started half way through the program instead of starting the whole run over. He set the numbers from the previous run printed out as initial conditions for the new run and realised something unexpected. Lorenz expected this new run to duplicate the old, however to his surprise, the new print out seemed completely different from the old yet he had not changed anything apart from the start up initial condition. All resemblance had disappeared [5]. In surprise with what he was seeing he performed accuracy checks on his inputs and the functionality of his machine and realised the difference was a result of slight difference in the initial conditions he had input. Lorenz had entered the shorter rounded-off numbers and the system responded sensitively with a different results [4]. Lorenz simplified his system down to a set of three nonlinear equations that described the currents induced in a convective cell of liquid when heated from the bottom [5]. Lorenz's discovery of chaos in his simple system of equations of only two nonlinearities awakened research into chaos. Scientists began to realise the existence of chaos in all aspect life. They identified chaos that develops in the heart of human, the main cause of

sudden and unexplained death, etc. James Gleick's book on Lorenz's discovery of chaos was amazingly a bestseller for months [16].
Chaos remains interesting and tremendously fascinating today. The Lorenz system of equations have generated a large interest for further studies. Today, there is numerous research on chaos, particularly, the Lorenz equations. Wilem Malkus invented the chaotic waterwheel, a mechanical analogous system which simulates the Lorenz equations in 1972 [10]. In 1975, Haken derives the Lorenz equations from a problem of irregular spiking in lasers [6], Knobloch discusses a derivation from a disc dynamo [8]. In 2013, Anthony Tongen, Roger J. Thelwell and David Becarra – Alonso studied a different version of the Wilem Malku's invention where they used sandwheel [17].

3. Methods Used

Dynamics is a field in mathematics which deals with change with systems that evolve in time. The subject analyses the behaviour of systems and discusses the questions of whether the system settle down to equilibrium, keeps repeating in cycles or does something more complicated [16]. Here, we discuss the tools we would need to comprehensively study the Lorenz system. We consider continuous autonomous dynamical systems. Details of the discussions here can be found in [16], [13], [7] and [12].

3.1. Linear System

The system of linear differential equations with n variables is stated as

$$\begin{aligned}\dot{x}_1 &= a_{1,1}x_1 + a_{1,2}x_2 + \cdots + a_{1,n}x_n\\ \dot{x}_2 &= a_{2,1}x_1 + a_{2,2}x_2 + \cdots + a_{2,n}x_n\\ &\vdots\\ \dot{x}_n &= a_{n,1}x_1 + a_{n,2}x_2 + \cdots + a_{n,n}x_n\end{aligned}$$

where all the $a_{i,j}$ are constant real numbers. This can be represented using the vector and matrix notation as

$$\dot{\mathbf{x}} = \mathbb{A}\mathbf{x} \tag{3.1}$$

where $\mathbb{A}$ is $n \times n$ matrix with given constant real entries $a_{i,j}$, and $\mathbf{x}$ is the column vector $\mathbb{R}^n$ of the variables,

$$\mathbf{x} = (x_1, \ldots, x_n)^T .$$

Theorem 3.1.1 (The Fundamental Theorem for Linear Systems) *Let $\mathbb{A}$ be $n \times n$ matrix. Then for a given $\mathbf{x}_0 \in \mathbb{R}^n$, the initial value problem*

$$\begin{aligned}\dot{\mathbf{x}} &= \mathbb{A}\mathbf{x}\\ \mathbf{x}(0) &= \mathbf{x}_0\end{aligned}$$

has solution given by

$$\mathbf{x}(t) = e^{At}\mathbf{x}_0$$

where e^{At} is an $n \times n$ matrix function defined by its Taylor series.

3.1.1. Linear System in $\mathbb{R}^2$

In this section we discuss the various phase portraits (geometric representation of solution curves) that are possible for the linear system (3.1). Before getting into detailed discussions, we state the following important theorem.

Theorem 3.1.2 (Linearity Principle) *Let equation (3.1) be a planar system. Suppose that* $\mathbf{y_1}(t)$ *and* $\mathbf{y_2}(t)$ *are solutions of this system, and that the vectors* $\mathbf{y_1}(0)$ *and* $\mathbf{y_2}(0)$ *are linearly independent. Then*

$$\mathbf{x}(t) = \alpha\mathbf{y_1}(t) + \beta\mathbf{y_2}(t)$$

is the unique solution of this system that satisfies $\mathbf{x}(0) = \alpha\mathbf{y_1}(0) + \beta\mathbf{y_2}(0)$.

Now consider the system (3.1) and suppose that $\mathbb{A}$ has two real eigenvalues $\lambda_1 < \lambda_2$. Assuming that $\lambda_i \neq 0$, there are three cases to consider:

(a) $\lambda_1 < 0 < \lambda_2$

(b) $\lambda_1 < \lambda_2 < 0$

(c) $0 < \lambda_1 < \lambda_2$

We give specific example of each case.

Example(saddle): Consider the simple case of the linear system (3.1) with

$$\mathbb{A} = \begin{pmatrix} \lambda_1 & 0 \\ 0 & \lambda_2 \end{pmatrix}.$$

The characteristic equation is

$$(\lambda - \lambda_1)(\lambda - \lambda_2),$$

so λ_1 and λ_2 are the eigenvalues with eigenvectors $(1, 0)$ and $(0, 1)$ respectively. From the Linearity principle, we find the general solution

$$\mathbf{x}(t) = \alpha e^{\lambda_1 t}\begin{pmatrix} 1 \\ 0 \end{pmatrix} + \beta e^{\lambda_2 t}\begin{pmatrix} 0 \\ 1 \end{pmatrix}.$$

Since $\lambda_1 < 0$, the straight-line solutions of the form $\alpha e^{\lambda_1 t}(1, 0)$ lie on the $x-$ axis and tend to $(0, 0)$ as $t \to \infty$. This axis is called the *stable line*. Since $\lambda_2 > 0$, the solutions $\beta e^{\lambda_2 t}(0, 1)$ lie on the $y-$ axis and tend away from $(0, 0)$ as $t \to \infty$; this axis is the *unstable line*. All solutions (with $\alpha, \beta \neq 0$) tend to ∞ in the direction of the unstable line, as $t \to \infty$, since $\mathbf{x}(t)$ comes closer and closer to $(0, \beta e^{\lambda_2 t})$ as t increases. In backward time, these solutions tend to ∞ in the direction of the stable line. The equilibrium point of a system of this type (eigenvalues satisfying $\lambda_1 < 0 < \lambda_2$) is called a *saddle*. see figure 3.1 for the phase portrait of this system.

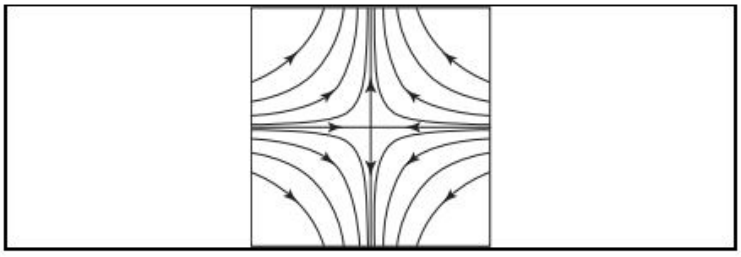

Figure 3.1: Saddle phase portrait for $x' = -x, y' = y$. Source [7].

Example: Consider the case where

$$\mathbb{A} = \begin{pmatrix} 1 & 3 \\ 1 & -1 \end{pmatrix}$$

The eigenvalues of $\mathbb{A}$ are ± 2. The eigenvector associated with $\lambda = 2$ is the vector $(3, 1)$; the eigenvector associated with $\lambda = -2$ is $(1, -1)$. The solution assumes the form

$$\mathbf{x}(t) = \alpha e^{2t} \begin{pmatrix} 3 \\ 1 \end{pmatrix} + \beta e^{-2t} \begin{pmatrix} 1 \\ -1 \end{pmatrix}$$

for some α, β. If $\alpha \neq 0$, as $t \to \infty$, we have

$$\mathbf{x}(t) \sim \alpha e^{2t} \begin{pmatrix} 3 \\ 1 \end{pmatrix} = \mathbf{x}_1(t)$$

whereas, if $\beta \neq 0$, as $t \to -\infty$,

$$\mathbf{x}(t) \sim \beta e^{-2t} \begin{pmatrix} 1 \\ -1 \end{pmatrix} = \mathbf{x}_2(t)$$

Thus, as time increases, the typical solution approaches $\mathbf{x_1}(t)$ while, as time decreases, this solution tends toward $\mathbf{x_2}(t)$, just as in previous example. See figure 3.2 for phase portrait.

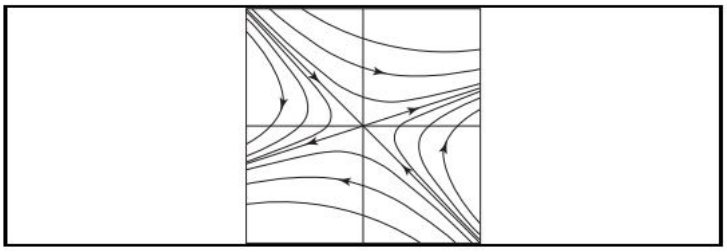

Figure 3.2: Saddle phase portrait for $x^{'} = x + 3y, y^{'} = x - y$. Source [7].

Example(Sink): Now consider the case where

$$\mathbb{A} = \begin{pmatrix} \lambda_1 & 0 \\ 0 & \lambda_2 \end{pmatrix}$$

but $\lambda_1 < \lambda_2 < 0$. The general solution assumes the form

$$\mathbf{x}(t) = \alpha e^{\lambda_1 t} \begin{pmatrix} 1 \\ 0 \end{pmatrix} + \beta e^{\lambda z t} \begin{pmatrix} 0 \\ 1 \end{pmatrix}$$

as before. Unlike the saddle case, now all solutions tend to (0.0) as $t \to \infty$. How then does it approach the origin? To answer this we compute the slope dy/dx of a solution with $\beta \neq 0$. We get

$$x(t) = \alpha e^{\lambda_1 t}$$
$$y(t) = \beta e^{\lambda_2 t}$$

and compute

$$\frac{dy}{dx} = \frac{dy/dt}{dx/dt} = \frac{\lambda_2 \beta e^{\lambda_2 t}}{\lambda_1 \alpha e^{\lambda_1 t}} = \frac{\lambda_2 \beta}{\lambda_1 \alpha} e^{(\lambda_2 - \lambda_1)t}.$$

Since $\lambda_2 - \lambda_1 > 0$, it follows that these slopes approach $\pm\infty$(provided $\beta \neq 0$). Thus, these solutions tend to the origin tangentially to the y-axis.
Since $\lambda_1 < \lambda_2 < 0$, we call λ_1 the stronger eigenvalue and λ_2 the weaker eigenvalue. The reason for this in this particular case is that the x-coordinates of solutions tend to 0 much more quickly that the y-coordinates. See figure 3.3a for phase portrait.

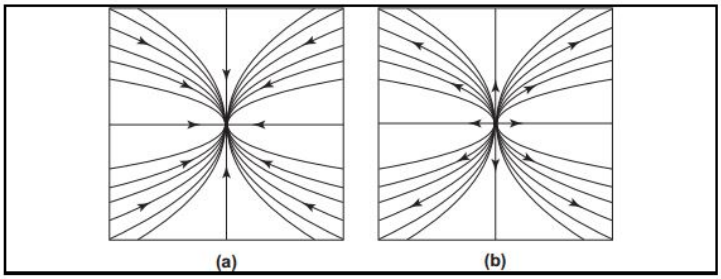

Figure 3.3: Phase portraits for a sink and a source. Source [7].

Example(Source): Consider the case when

$$\mathbb{A} = \begin{pmatrix} \lambda_1 & 0 \\ 0 & \lambda_2 \end{pmatrix}$$

which satisfies $0 < \lambda_2 < \lambda_1$. The general solution and phase portrait remain the same, except that all solutions now tend away from $(0, 0)$ along the same paths. See figure 3.3b.

Next we consider the case where the roots of the characteristic polynomial are complex numbers. In such case, we no longer have straight-line solutions. However, we can still derive the general solution as before by using a few tricks involving complex numbers and functions.
Example(Center): Consider the case where

$$\mathbb{A} = \begin{pmatrix} 0 & \beta \\ -\beta & 0 \end{pmatrix}$$

and $\beta \neq 0$. The characteristic polynomial is $\lambda^2 + \beta^2 = 0$, with eigenvalues now imaginary numbers $\pm i\beta$. We find the corresponding eigenvector to be $\lambda = i\beta$ by solving

$$\begin{pmatrix} -i\beta & \beta \\ -\beta & -i\beta \end{pmatrix} \begin{pmatrix} x \\ y \end{pmatrix} = \begin{pmatrix} 0 \\ 0 \end{pmatrix}$$

or $i\beta x = \beta y$, since the second equation is redundant. Thus, we find a complex eigenvector $(1, i)$, and so the system assumes solution of the form

$$\mathbf{x}(t) = e^{i\beta t} \begin{pmatrix} 1 \\ i \end{pmatrix}.$$

Using Euler's formula:

$$e^{i\beta t} = \cos \beta t + i \sin \beta t,$$

we rewrite the solution as

$$\mathbf{x}(t) = \begin{pmatrix} \cos \beta t + i \sin \beta t \\ i(\cos \beta t + i \sin \beta t) \end{pmatrix} = \begin{pmatrix} \cos \beta t + i \sin \beta t \\ -\sin \beta t + i \cos \beta t \end{pmatrix}$$

This can further be written as

$$\mathbf{x}(t) = \mathbf{x}_{re}(t) + i\mathbf{x}_{im}(t)$$

where

$$\mathbf{x}_{re}(t) = \begin{pmatrix} \cos\beta t \\ -\sin\beta t \end{pmatrix}, \mathbf{x}_{im}(t) = \begin{pmatrix} \sin\beta t \\ \cos\beta t \end{pmatrix}$$

But now we see that both $\mathbf{x}_{re}(t)$ and $\mathbf{x}_{im}(t)$ are real solutions of the original system. We smply check

$$\begin{aligned} \mathbf{x}'_{re}(t) + i\mathbf{x}'_{im}(t) &= \mathbf{x}'(t) \\ &= \mathbb{A}\mathbf{x}(t) \\ &= \mathbb{A}\left(\mathbf{x}_{re}(t) + i\mathbf{x}_{im}(t)\right) \\ &= \mathbb{A}\mathbf{x}_{re} + i\mathbb{A}\mathbf{x}_{im}(t) \end{aligned}$$

Equating the real and imaginary parts of this equation yields $\mathbf{x}'_{re} = \mathbb{A}\mathbf{x}_{re}$ and $\mathbf{x}'_{im} = \mathbb{A}\mathbf{x}_{im}$ which shows that both are indeed solutions. Since

$$\mathbf{x}_{re}(0) = \begin{pmatrix} 1 \\ 0 \end{pmatrix}, \mathbf{x}_{im}(0) = \begin{pmatrix} 0 \\ 1 \end{pmatrix}$$

the linear combination of these solutions,

$$\mathbf{x}(t) = a_1\mathbf{x}_{re}(t) + c_2\mathbf{x}_{im}(t)$$

where c_1 and c_2 are arbirary constants, provides a solution to any initial value problem. Each of these solutions is a periodic function with period $2\pi/\beta$. The phase portrait shows that all solutions lie on circles centered at the origin. These circles are traversed in the clockwise direction if $\beta > 0$, counterclockwise if $\beta < 0$. See figure 3.4. This type of system is called a *center*.

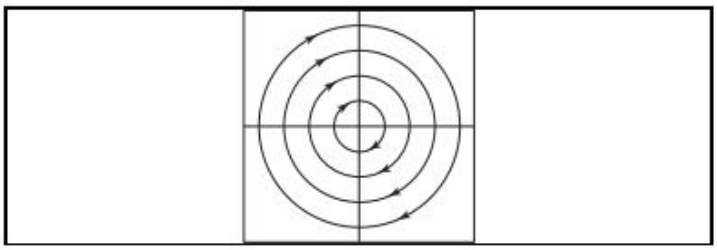

Figure 3.4: Phase portraits for a center. Source [7].

Theorem 3.1.3 (Stability of Linear Systems) *Let $\delta = \det \mathbb{A}$ and $\tau = \text{trace } \mathbb{A}$ and consider the linear system (3.1) in $\mathbb{R}^2$*

(a) If $\delta < 0$ then equation (3.1) has a saddle at the origin.

(b) If $\delta > 0$ and $\tau^2 - 4\delta \geq 0$ then equation (3.1) has a node (sink) at the origin; it is stable if $\tau < 0$ and unstable if $\tau > 0$

(c) If $\delta > 0$, $\tau^2 - 4\delta < 0$ and $\tau \neq 0$ then (3.1) has a focus at the origin; it is stable if $\tau > 0$ and unstable if $\tau > 0$.

(d) If $\delta > 0$ and $\tau = 0$ then equation (3.1) has a centre at the origin.

Remark: Note that in the case (b), $\tau^2 \geq 4|\delta| > 0$; i.e., $\tau \neq 0$

3.2. Nonlinear System

The nonlinear system of differential equations is stated as

$$\dot{\mathbf{x}} = f(\mathbf{x}) \tag{3.2}$$

where $f : E \to \mathbb{R}^n$ and E is a subset of $\mathbb{R}^n$. Nonlinear systems in general, are difficult to solve analytically, however, we are able to study the behaviour of the system and extract most necessary information with geometrical techniques, topological techniques and numerical methods. It is neccessary to define some terminologies and notation concerning the derivative Df of a function $f : \mathbb{R}^n \to \mathbb{R}^n$.

Definition 3.2.1 *The function $f : \mathbb{R}^n \to \mathbb{R}^n$ is differentiable at $\mathbf{x}_0 \in \mathbb{R}^n$ if there is a linear transformation $Df(\mathbf{x_0}) \in L(\mathbb{R}^n)$(linear space), that satisfies*

$$\lim_{|h|\to 0} \frac{|f(x_0 + h) - f(x_0) - Df(x_0)\, h|}{|h|} = 0.$$

The linear transformation $Df(x_0)$ is called the derivative of f at $\mathbf{x_0}$. The following theorem gives us a method for computing the derivative in coordinates.

Theorem 3.2.1 *If $f : \mathbb{R}^n \to \mathbb{R}^n$ is differentiable at $\mathbf{x}_0$, then the partial derivatives $\partial f_i/\partial x_j, i, j = 1, \ldots, n$ all exist at $\mathbf{x}_0$ and for all $\mathbf{x} \in \mathbb{R}^n$,*

$$Df(\mathbf{x}_0)\,\mathbf{x} = \sum_{j=1}^{n} \frac{\partial f}{\partial x_j}(\mathbf{x}_0)\, x_j.$$

Thus, if f is a differentiable function, the derivative Df is given by the Jacobian matrix

$$Df = \left[\frac{\partial f_i}{\partial x_j}\right].$$

Theorem 3.2.2 (The Fundamental Existence-Uniqueness Theorem) *Let E be an open subset of $\mathbb{R}^n$ containing $\mathbf{x}_0$ and assume that $f \in C^1(E)$. Then there exists an $a > 0$ such that the initial value problem*

$$\begin{aligned} \dot{\mathbf{x}} &= f(\mathbf{x}) \\ \mathbf{x}(0) &= \mathbf{x}_0 \end{aligned}$$

has a unique solution $\mathbf{x}(t)$ on the interval $[-a, a]$.

Definition 3.2.2 *The function $\phi(t; \mathbf{x}_0)$, which gives the solution as a function of the time t and initial condition $\mathbf{x}_0$, is called the flow of the differential equation (3.2).*

3.3. Linearization

A very important state of our system of differential equations is the stationary state. This is the point where $\dot{\mathbf{x}} = 0$. Thus, there is no flow at this point.

Definition 3.3.1 *A point* $\mathbf{x}_0 \in \mathbb{R}^n$ *is called an equilibrium point or critical point of equation (3.2) if* $f(\mathbf{x}_0) = 0$. *An equilibrium point* $\mathbf{x}_0$ *is called a hyperbolic equilibrium point of equation (3.2) if none of the eigenvalues of the matrix* $Df(\mathbf{x}_0)$ *have zero real part.*

After obtaining the equilibrium points, we would want to know how the system behaves close to the equilibriums. This leads us to what is called linearization. The local behaviour of the nonlinear system (3.2) near a hyperbolic equilibrium point $\mathbf{x}_0$ is qualitatively determined by the behaviour of the linear system

$$\dot{\mathbf{x}} = \mathbb{A}\mathbf{x} \tag{3.3}$$

with the matrix $\mathbb{A} = Df(\mathbf{x}_0)$, near the origin. If $\mathbf{x}_0$ is an equilibrium point of equation (3.2), then $f(0) = 0$ and by Taylor's Theorem,

$$\mathbf{f}(\mathbf{x}) = D\mathbf{f}(\mathbf{0})\mathbf{x} + \frac{1}{2}D^2\mathbf{f}(\mathbf{0})(\mathbf{x}, \mathbf{x}) + \cdots .$$

It follows that the linear function $Df(0)\mathbf{x}$ is a good first approximation to the nonlinear function $f(\mathbf{x})$ near $\mathbf{x} = 0$ and it is reasonable to expect that the behavior of the nonlinear system (3.2) near the point $\mathbf{x}$ will be approximated by the behaviour of its linearization at $\mathbf{x} = 0$.

Definition 3.3.2 *An equilibrium point* $\mathbf{x}_0$ *of equation (3.2) is called a sink if all the eigenvalues of the matrix* $Df(\mathbf{x}_0)$ *have negative real part; it is called a source if all the eigenvalues of* $Df(\mathbf{x}_0)$ *have positive real parts; and it is called a saddle if it is a hyperbolic equilibrium point and* $Df(\mathbf{x}_0)$ *has at least one eigenvalue with a positive real part and at least one with a negative real part.*

3.4. Stability of Nonlinear System

After a "small" perturbation of the system, does the system decay (returns to its equilibrium point) or grows and if it does, how fast is it? The following definition explains the meaning of stability, unstable, asymptotically stable and global stability.

Definition 3.4.1 *Let* $\phi(t; \mathbf{x})$ *denote the flow of differential equation (3.2) defined for all* $t \in \mathbb{R}$. *An equilibrium point* $\mathbf{x}_0$ *of equation (3,2) is stable if for all* $\epsilon > 0$ *there exists a* $\delta > 0$ *such that for* $\mathbf{x} \in N_\delta(\mathbf{x}_0)$ *and* $t \geq 0$ *we have*

$$\phi(t; \mathbf{x}) \in N_\varepsilon(\mathbf{x}_0) .$$

The equilibrium point $\mathbf{x}_0$ *is unstable if it is not stable. And* $\mathbf{x_0}$ *is asymptotically stable if it is stable and if there exists a* $\delta > 0$ *such that for all* $\mathbf{x} \in N_\delta(\mathbf{x}_0)$ *we have*

$$\lim_{t\to\infty} \phi(t; \mathbf{x}) = \mathbf{x}_0.$$

If the flow approaches $\mathbf{x}^*$ *from all initial conditions,* $\mathbf{x}^*$ *is said to be globally stable.*

These information are obtained from the linearized system, thanks to the Hartman-Grobman Theorem. The stability of any hyperbolic equilibrium point $\mathbf{x}_0$ of equation (3.2) is determined by the signs of the real parts of the eigenvalues λ_j of the Jacobian matrix. This is summarised in the following theorem:

Theorem 3.4.1 (Hartman-Grobman Theorem of Stability) *Let $J = Df(\mathbf{x}_0)$ be the Jacobian matrix for the system (3.2) evaluated at a fixed point $\mathbf{x}_0$ and let λ_j be its eigenvalues*

(a) If $\Re(\lambda_j) < 0$ for all λ_j then the fixed point $\mathbf{x}_0$ is asymptotically stable.

(b) If $\Re(\lambda_j) > 0$ for at least one λ_j, then the fixed point $\mathbf{x}_0$ is unstable.

(c) If $\Re(\lambda_j) = 0$ for at least one λ_j, then the fixed point $\mathbf{x}_0$ is nonhyperbolic and its stability cannot be determined by the linearization method.

From the theorem above, any *hyperbolic equilibrium point of equation (3.2) is either asymptotically stable or unstable.* Therefore, the only time that an equilibrium point $\mathbf{x}_0$ of equation (3.2) can be stable but not asymptotically stable is when $Df(\mathbf{x}_0)$ has a zero eigenvalue or a pair of complex-conjugate, pure-imaginary eigenvalues $\lambda = \pm b$.
In the case of nonhyperbolic equilibrium point, we need the Lyapunov theorem which follows.

Theorem 3.4.2 (Lyapunov Theorem) *Let E be an open subset $\mathbb{R}^n$ containing $\mathbf{x}_0$. Suppose that $f \in C^1(E)$ and that $f(\mathbf{x}_0) = 0$. Suppose further that there exists a real valued function $V \in C^1(E)$ satisfying $V(\mathbf{x}_0) = 0$ and $V(x) > 0$ if $x \neq \mathbf{x}_0$. Then*

(a) If $\dot{V}(x) \leq 0$ for all $x \in E$, $\mathbf{x}_0$ is stable;

(b) If $\dot{V}(x) < 0$ for all $x \in E \backslash \{\mathbf{x}_0\}$, $\mathbf{x}_0$ is asymptotically stable;

(c) If $\dot{V}(x) > 0$ for all $x \in E \backslash \{\mathbf{x}_0\}$, $\mathbf{x}_0$ is unstable.

In many applications, computing the eigenvalues of the system for stability study is difficult. For instance, in the Lorenz system we would be studying, computing the eigenvalues for the Rayleigh number, $r > 1$ would not be helping. In such cases the characteristic polynomial can save us from complex computation. For instance we can determine the signs of the possible zeros which gives the nature of stability of the eigenvalues. Descartes' rule of signs gives an idea of the zeros of a polynomial function e.g. the number of positive zeros, negatives zeros and even the possible number of imaginary solutions. Of course, we cannot leave out the well-known and mostly used Routh-Hurwitz stability criterion in such situations.

3.4.1. The Routh-Hurwitz Stability Criterion

The Routh-Hurwitz stability criterion as proved independently by A. Hurwitz and E. J. Routh has occupied the interest of many engineers for investigating the stability of linear systems. The Routh - Hurwitz criterion is a necessary and sufficient criterion for the stability of linear systems. Consider the characteristic polynomial:

$$q(s) = a_n s^n + a_{n-1} s^{n-1} + \cdots + a_1 s + a_0 = 0$$

It is necessary but not sufficient requirement that all the coefficients for a stable system be nonzero. If this is not satisfied, we conclude immediately that the system is unstable. However, if they are satisfied we proceed to ascertain the stability of the system.

The algorithm for the Routh-Hurwitz criterion begins with ordering the characteristic polynomial into the following array

$$\begin{array}{c|ccc} s^n & a_n & a_{n-2} & a_{n-4}\cdots \\ s^{n-1} & a_{n-1} & a_{n-1} & a_{n-5}\cdots \end{array}$$

Further rows of the array are then completed as

$$\begin{array}{c|ccc} s^n & a_n & a_{a-2} & a_{a-4} \\ s^{n-1} & a_{n-1} & a_{a-3} & a_{n-5} \\ s^{n-2} & b_{n-1} & b_{a-3} & b_{n-5} \\ s^{n-3} & c_{n-1} & c_{n-3} & n_{n-5} \\ \vdots & \vdots & \vdots & \vdots \\ s^0 & h_{n-1} & & \end{array}$$

where

$$b_{n-1} = \frac{a_{n-1}a_{n-2} - a_n a_{n-3}}{a_{n-1}} = \frac{-1}{a_{n-1}} \begin{vmatrix} a_n & a_{n-2} \\ a_{n-1} & a_{n-1} \end{vmatrix}$$

$$b_{n-3} = -\frac{1}{a_{n-1}} \begin{vmatrix} a_n & a_{n-1} \\ a_{n-1} & a_{n-5} \end{vmatrix}$$

$$c_{\mathrm{a}-1} = \frac{-1}{b_{n-1}} \begin{vmatrix} a_{n-1} & a_{n-1} \\ b_{2-1} & b_{n-1} \end{vmatrix}$$

The Routh-Hurwitz criterion states that the number of roots of $q(s)$ with positive real parts is equal to the number of change in sign of the first column of the Routh array. For stability, we require that no changes in the first column of the Routh array. We discuss two special cases of the Routh-Hurwitz criterion with illustrative examples.

Case 1. There is a zero in the first column, but some other elements of the row containing the zero in the first column are nonzero. If only one element in the array is zero, it may be replaced with a small positive number, ϵ, and the limit as it approaches zero is taken after completing the array. For example, consider the characteristic polynomial:

$$q(s) = s^5 + 2s^4 + 2s^3 + 4s^2 + 11s + 10$$

The Routh array is then

$$\begin{array}{c|c|c|c} s^5 & 1 & 2 & 11 \\ s^4 & 2 & 4 & 10 \\ s^3 & \epsilon & 6 & 0 \\ s^2 & c_1 & 10 & 0^* \\ s^1 & d_1 & 0 & 0 \\ s^0 & 10 & 0 & 0 \end{array}$$

where

$$c_1 = \frac{4\epsilon - 12}{\epsilon} = \frac{-12}{\epsilon}$$

and

$$d_1 = \frac{6c_1 - 10\epsilon}{c_1} \to 6$$

The signs changes from ϵ to c_1 and to d_1 as we move down the first column. We conclude that the system is unstable, and two zeros lie in the right half of the plane.

Case 2. There is a zero in the first column, and the other elements of the row containing the zero are also zero. This is the case when all the elements in one row are zero or when the row consists of a sigle element that is zero. This case is realised when the polynomial contains roots that are symmetrically located about the origin of the s plane. Thus, this is the case when factor $(s+\sigma)(s-\sigma)$ or $(s+\omega i)(s-\omega i)$ occur. In such cases, we make use of what is called **auxiliary polynomial**, $U(s)$, which immediately preceds the zero entry in the Routh array. The order of the auxiliary polynomial is always even and indicates the number of symmetrical root pairs.
Example Consider the characteristic polynomial

$$q(s) = s^3 + 2s^2 + 4s + K$$

where K is free. The Routh array is

$$\begin{array}{c|cc} s^3 & 1 & 4 \\ s^2 & 2 & K \\ s^1 & \frac{8-K}{2} & 0 \\ s^0 & K & 0 \end{array}$$

From the Routh-Hurwitz stability criterion, stability of the system requires that

$$0 < K < 8$$

however, when $K = 8$, we obtain the case of marginal stability with two roots on the ωi-axis. For $K = 0$, we form the auxiliary polynomial form the preceding row s^2 -row. Notice the even power.

$$U(s) = 2s^2 + Ks^0 = 2s^2 + 8 = 2\left(s^2 + 4\right) = 2(s + 2i)(s - 2i)$$

dividing $q(s)$ by $U(s)$ tells us that the auxiliary polynomial, $U(s)$ is indeed a factor of the characteristic polynomial. And so, when $K = 8$, the characteristic polynomial has the factors

$$q(s) = (s + 2)(s + 2i)(s - 2i)$$

3.4.2. Descartes' rule of signs

The Descartes rule of signs as earlier said gives an idea of the zeros of a polynomial function.

Theorem 3.4.3 (Descartes' rule of signs) *Let $p(x) = a_0x^{b_0} + a_1x^{b_1} + \cdots + a_nx^{b_n}$ denote a polynomial with nonzero real coefficients a_i, where the b_i, are integers satisfying $0 \leq b_0 < b_1 < b_2 < \ldots < b$. Then the number of positive real zeros of $p(x)$ (counted with multiplicities) is either equal to the number of variations in sign in the sequence $(a_0, \cdots a_n)$ of the coefficients or less than it by an even whole number. The number of negative zeros of $p(x)$ (counted with multiplicities) is either equal to the number of variations in sign in the sequence of the coefficients of $p(-x)$ or less than it by an even whole number.*

Example: For the polynomial function

$$f(x) = x^3 - 2x^2 - x + 2$$

we want to find the number of positive, negative or imaginary solutions. From the function $f(x)$ we observe two sign changes. According to the rules, the number of positive zeros is either equal to the number of sign change of $f(x)$ or could be less than a positive even integer. Therefore the function may have either two or zero i.e., $2 - 2 = 0$ possible roots. For the negative possible roots, we check

$$\begin{aligned} f(-x) &= (-x)^2 - 2(-x)^2 - (-x) + 2 \\ &= x^2 - 2x^2 + x + 2 \end{aligned}$$

Again the number of negative zeros is equal to the number of sign changes or less by a positive even integer. Here the only possible number of negative root is one, because $1-2 = -1$ does not make sense. The function is a $3rd$-order polynomial, hence we expect three roots. With this information, we can generate the following possibilities:

Positive	*Negative*	*Imaginary*	*Total*
2	1	0	3
0	1	2	3

3.5. Bifurcation

Perturbation of a dynamical system cannot only change the stability of the equilibrium points, but also the qualitative structure of the system. These qualitative changes in the dynamics are called bifurcations, and the parameter values at which they occur are called bifurcation point. This is very common in application, where we would want to see how *control parameters* affect stability and instability of the system as they vary. There are several types of bifurcation that a dynamical system could experience. These include the Pitchfork bifurcation and the Andronov - Hopf bifurcation which the Lorenz system experiences.

The pitchfork bifurcation is prevalent in systems which are symmetric such as the Lorenz system. There are two types of this bifurcation, the subcritical pitchfork bifurcation and supercritical pitchfork bifurcation. Supercritical pitchfork bifurcation normally are formed in systems where new stable equilibria are created to add to an existing stable equilibrium point as the system varies through a bifurcation value. The already existing equilibrium point becomes unstable after bifurcation. This is not so different from the subcritical pitchfork bifurcation except that the newly born equilibria are unstable in this case.

In the Andronov – Hopf bifurcation, no new equilibria arise. Instead, a periodic solution is born at the equilibrium point as the control parameter varies through the bifurcation value. This type of bifurcation is experienced by systems where equilibrium point has complex eigenvalues. There are also two types of this bifurcation, the Hopf supercritical bifurcation and subcritical Hopf bifurcation. At supercritical Hopf bifurcation, limit cycle appears after the real part of the eigenvalue has become positive, whereas limit cycle appears before the bifurcation, where the real part of the eigenvalue at the fixed point is negative in the case of Hopf subcritical bifurcation. See [13] for detailed discussions.

The Homoclinic bifurcation is one of the kinds of **gobal bifurcations**. In this bifurcation, a periodic orbit or cycle is born or dies in a homoclinic loop as it moves close and touch a saddle point. If $\phi(t;\mathbf{x})$ tends to the equilibrium point $\mathbf{x}^*$ as $t \to \pm\infty$, then $\phi(t;\mathbf{x})$ is a homoclinic orbit. More precisely, a homoclinic orbit lies in the intersection of the *stable manifold* and the *unstable manifold*. For a clearer understanding of homoclinic bifurcation, we demostrate with the following example. Consider the system

$$\begin{aligned}\dot{x} &= y\\ \dot{y} &= \mu y + x - x^2 - xy\end{aligned}$$

The system has bifurcation at $\mu_c \approx -0.8645$. For $\mu < \mu_c$, a stable limit cycle passes close to a saddle point at the origin. See figure 3.5a. As μ increases to μ_c, the limit cycle swells (see figure 3.5b) and enters into the saddle, resulting in a homoclinic orbit. See figure 3.5c. When $\mu > \mu_c$, the saddle connection breaks and the loop is destroyed, see figure 3.5d.

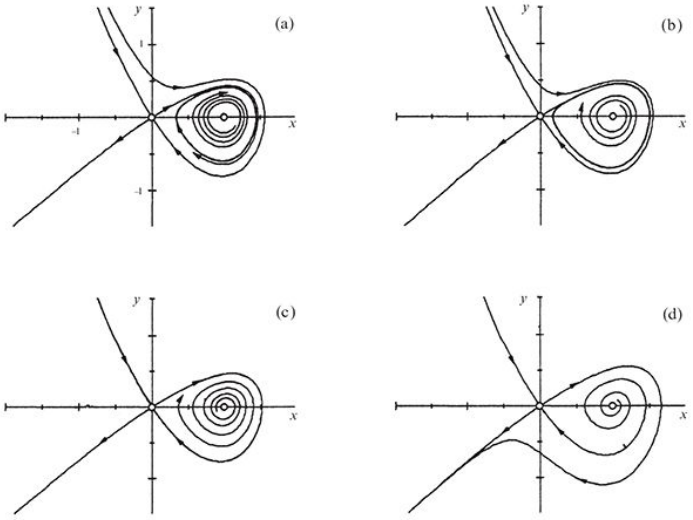

Figure 3.5: Homoclinic bifurcation through $\mu_c \approx -0.8645$. Source [16].

3.6. Limit Sets and Attractors

The long – term behaviour of the flow $\phi(t;\mathbf{x}_0)$ of a dynamical system as time goes to plus or minus infinity is key. We first explain the concept of ω- limit set and the α- limit set of $\phi(t;\mathbf{x}_0)$.

Definition 3.6.1 *A point* $\mathbf{q}$ *is an* ω*- limit point of the trajectory of* $\mathbf{x}_0$*, provided that* $\phi(t;\mathbf{x}_0)$ *keeps coming near* $\mathbf{q}$ *as* t *goes to infinity, i.e., there is a sequence of times* t_j*, with* t_j *going to infinity as* j *goes to infinity, such that* $\phi(t_j;\mathbf{x}_0)$ *converges to* $\mathbf{q}$*. Certainly, if* $\|\phi(t;\mathbf{x}_0) - x^*\| \to 0$ *as* $t \to \infty$ *then* x^* *is the only* ω*- limit point of* $\mathbf{x}_0$*. There can be more than one point that is an* ω*-limit point of* $\mathbf{x}_0$*. The set of all* ω*-limit points of* $\mathbf{x_0}$ *is denoted by* $\omega(\mathbf{x_0})$ *and is called the* $\omega - limitset$ *of* $\mathbf{x_0}$*.*
Similarly, a point $\mathbf{q}$ *is an* $\alpha-$ *limit point of* $\mathbf{x_0}$*, provided that* $\phi(t;\mathbf{x}_0)$ *keeps coming near* $\mathbf{q}$ *as* t *goes to minus infinity. In particular, if* $\|\phi(t;\mathbf{x}_0) - x^*\| \to 0$ *as* $t \to -\infty$*, then* x^* *is*

the only α- limit point of $\mathbf{x}_0$. The set of all α-limit points of $\mathbf{x_0}$ is denoted by $\alpha(\mathbf{x_0})$ and is called the α- limit set of $\mathbf{x_0}$.

Remark: if $\mathbf{x_0}$ is a fixed point, then $\omega(\mathbf{x_0}) = \alpha(\mathbf{x_0}) = \{\mathbf{x_0}\}$

Definition 3.6.2 *Let $\phi(t;\mathbf{x}_0)$ be the flow of system of differential equations (3.2). A subset of the phase space S is called positive invariant provided that $\phi(t;\mathbf{x}_0)$ is in S for all $\mathbf{x}_0$ in S and all $t \geq 0$. A subset of the phase space S is called negatively invariant provided that $\phi(t;\mathbf{x}_0)$ is in S for all $\mathbf{x_0}$ in S and $t \leq 0$. Finally, a subset of the phase space S is called invariant provided that $\phi(t;\mathbf{x}_0)$ is in S for all $\mathbf{x}_0$ in S and all real t.*

An invariant set S is called *transitive*, provided that there is a point $\mathbf{x}_0$ in S such that the orbit of $\mathbf{x}_0$ comes arbitrarily close to every point in S.

3.7. Periodic Orbits

The flow $\phi(t;\mathbf{x}_0)$ of the differential equation (3.2) may be periodic. A point $\mathbf{x}_0$ is a *periodic point of period* T if $\phi(T;\mathbf{x}_0) = \mathbf{x}_0$,but $\phi(t;\mathbf{x}_0) \neq \mathbf{x}_0$ for $0 < t < T$. The set of all the points $\{\phi(t;\mathbf{x}_0) = \mathbf{x}_0 : 0 \leq t \leq T\}$ is called a *periodic orbit* or *closed orbit* if $\mathbf{x}_0$ is periodic with period T. The flow $\phi(t;\mathbf{x}_0)$ is periodic in time, thus $\phi(t+T;\mathbf{x}_0) = \phi(t;\mathbf{x}_0)$ for all t, hence the name periodic orbit. Also, the set of points on the whole orbit $\{\phi(t;\mathbf{x}_0) := -\infty < t < \infty\}$ is a closed set, thus the orbit "closes" up, hence the name closed orbit. Orbits close to periodic orbits may not be periodic. In such case, we have what is called *limit cycle*. A limit cycle is an isolated periodic orbit. As in the case of periodic orbits, limit cycles can have different types of stability depending on trajectories close to the periodic orbit move towards or away from it.

3.8. Poincaré Map

The Poincare map also referred to as the first return map is a type of map for analysing systems that appear to have periodic behaviour.

Definition 3.8.1 *Consider a system of differential equations (3.2), and a point $\mathbf{x}^*$ for which one of the coordinate functions $f_k(\mathbf{x}^*) \neq 0$. The hyperplane through $\mathbf{x}^*$ formed by setting the k^{th} coordinate equal to a constant,*

$$\Sigma = \{\mathbf{x} : x_k = x_k^*\}$$

is called a transversal, because trajectories are crossing it near $\mathbf{x}^*$. Assume that $\phi(\tau^*;\mathbf{x}^*)$ is again in Σ for some $\tau^* > 0$. We also assume that there are no other intersections of $\phi(t;\mathbf{x}^*)$ with Σ near $\mathbf{x}^*$. For $\mathbf{x}$ near $\mathbf{x}^*$, there is a nearby time $\tau(\mathbf{x})$ such that $\phi(\tau(\mathbf{x});\mathbf{x})$ is in Σ. Then,

$$\mathbb{P}(\mathbf{x}) = \phi(\tau(\mathbf{x});\mathbf{x})$$

is the Poincaré map.

In the following theorem, we compare the eigenvalues of the Poincaré map with the eigenvalues of the period map of the flow.

Theorem 3.8.1 *Assume that* $\mathbf{x}^*$ *is on a periodic orbit with period* T*. Let* Σ *be a hyperplane through* $\mathbf{x}^*$*, formed by setting one of the variables equal to a constant; that is, for some* $1 \leq k \leq n$ *with* $f_k(\mathbf{x}^*) \neq 0$*, let*

$$\Sigma = \{\mathbf{x} : x_k = x_k^*\}$$

Let $\mathbb{P}$ *be the Poincaré map from a neighborhood of* $\mathbf{x}^*$ *in* Σ *back to* Σ*. Then, the* n *eigenvalues of* $D_{\mathbf{x}}\phi_{(T;\mathbf{x}^*)}$ *consist of the* $(n-1)$ *eigenvalues of* $D\mathbb{P}_{(\mathbf{x}^*)}$*, together with 1, the latter resulting from the periodicity of the orbit.*

3.9. Chaotic Attractors

The name chaotic attractors has been chosen to describe limit sets that exhibit a complicated properties such as *sensitivity dependence on initial conditions*. There is no one single definition for chaos. However, all definitions for a chaotic system have one common feature which sensitive dependence on initial conditions.

Definition 3.9.1 *A chaotic attractor is a transitive attractor* $\mathbb{A}$ *for which the flow has sensitive dependence on initial conditions when restricted to* $\mathbb{A}$ *[13].*

Strogatz [16] also defines chaos as follows:

Definition 3.9.2 *Chaos is aperiodic long-term behaviour in a deterministic system that exhibits sensitive dependence on intial conditions.*

Remarks: "Aperiodic long-term behaviour" means that trajectories which do not settle down to fixed points, periodic orbits, quasiperiodic orbits as $t \to \infty$.
"Deterministic" means that the system has no random or noisy input or parameters. The irregularity arises from the nonlinear components of the system rather than noisy driving forces.
"Sensitive dependence on initial conditions" means that nearby trajectories separate exponentially fast.

4. The Lorenz Equations

The Lorenz equations are given by

$$\begin{aligned} \dot{x} &= \sigma(y - x) \\ \dot{y} &= rx - y - xz \\ \dot{z} &= xy - bz. \end{aligned} \tag{4.1}$$

The parameters σ, r, and b are positive. Lorenz found these equations to model convective rolls in the atmosphere in his research to find a mathematical model that could predict the weather. Lorenz identified the parameter values $\sigma = 10, b = 8/3$ and $r = 28$ where the equations reveal a strange behaviour. In this section, we study the properties and dynamics of the Lorenz equations with the Lorenz parameter values $\sigma = 10, b = 8/3$ and r as a control parameter. The Lorenz equations have only two nonlinearities, the quadratic terms xy and xz. The system is deterministic without any stochastic input, however, it exhibits complicated dynamic and random behaviour. See figure 4.1. The trajectory is regular up to $t = 18$, after which it becomes completely random for all future times. The Lorenz system is sensitive to initial conditions. In figure 4.2, we show the

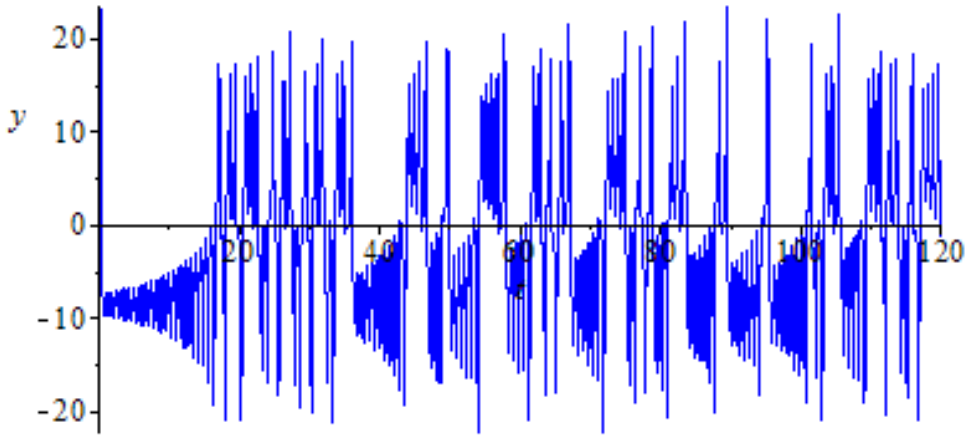

Figure 4.1: Random behaviour of the Lorenz system.

time series plot for x and t for the initial conditions $x(0) = y(0) = z(0) = 1$ (in blue) and $x(0) = 1.001, y(0) = 1, z(0) = 1$ (in green). This reveals how 0.1 percent change in the initial condition of the x variable makes a big difference in the solution. The two x solutions are quite the same until at $t = 10$ after which they behave completely different. At $t = 11$, we observe that the two solutions are on different sides. Lorenz called this property "The butterfly effect", which is a basic property of chaotic systems. The system has a natural symmetry $(x, y, z) \to (-x, -y, z)$. Replacing $(x, y) \to (-x, -y)$ does not change anything in the equation. Therefore, if $(x(t), y(t), z(t))$ is a solution, then so is $(-x(t), -y(t), z(t))$. Generally, all solutions are either symmetric themselves,

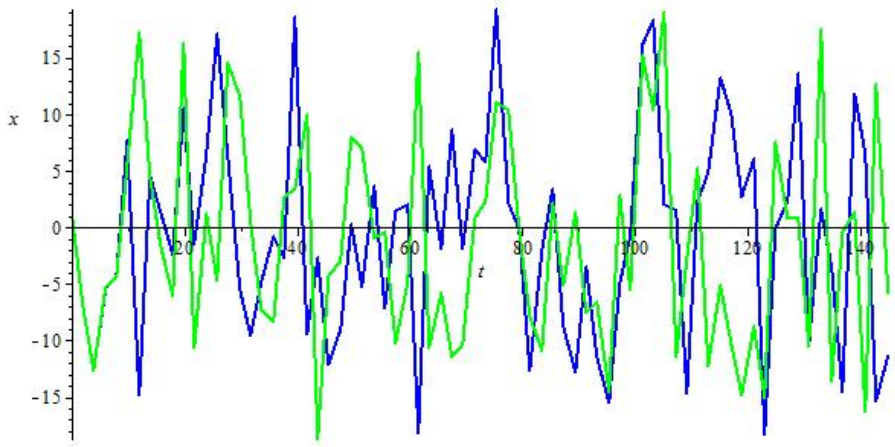

Figure 4.2: Time series plot for x and t for the initial conditions $x(0) = y(0) = z(0) = 1$ (in blue) and $x(0) = 1.001, y(0) = 1, z(0) = 1$ (in green).

or have a symmetric partner. This can be shown by a simple substitution of the above transformation in the Lorenz equations,

$$\begin{aligned} -\dot{x} &= \sigma(-(-x) + (-y)) \Rightarrow \frac{dx}{dt} = \sigma(y - x) \\ -\dot{y} &= r(-x) - (-y) - (-x)z \Rightarrow \frac{dy}{dt} = x(r - z) - y \\ -\dot{z} &= -b(z) + (-x)(-y) \Rightarrow \frac{dz}{dt} = xy - bz. \end{aligned}$$

The z-axis, $x = 0 = y$ is invariant. All trajectories which start on the z-axis remain on it and tend towards the origin $(0, 0, 0)$. See definition 3.6.2.

4.1. Stationary Points

The system has two types of stationary points:

1. $(x^*, y^*, z^*) = (0, 0, 0)$. The origin is a fixed point for all values of the parameter.
2. $x^* = y^* = \pm\sqrt{b(r-1)}, z^* = r - 1$, the symmetric pair C^+ and C^-.

4.2. Stability of the Origin

The linearized system is

$$\begin{aligned} \dot{x} &= \sigma(y - x) \\ \dot{y} &= rx - y \\ \dot{z} &= -bz. \end{aligned}$$

The equation for z is decoupled with solution $z(t) = e^{-bt}$. This shows that $z(t)$ approaches zero exponentially fast. The other two directions are governed by the system

$$\begin{pmatrix} \dot{x} \\ \dot{y} \end{pmatrix} = \begin{pmatrix} -\sigma & \sigma \\ r & -1 \end{pmatrix} \begin{pmatrix} x \\ y \end{pmatrix}$$

We can determine the nature and stability by definition 3.3.2 and theorem 3.4.1. The trace $\tau = -\sigma - 1 < 0$ and determinant $\Delta = \sigma(1-r)$, hence the origin is saddle point if $r > 1$. However, the system is three-dimensional and so this is a *new type of saddle* [16]. Now we have z decaying to the origin and the other two directions moving in opposite direction in respect to the origin. Also, $\tau^2 - 4\Delta = (\sigma+1)^2 - 4\sigma(1-r) = (\sigma+1)^2 + 4\sigma r > 0$, and so we have stable node if $r < 1$ since all directions are sinking to the origin. The eigenvalues are of the system's Jacobian evaluated at the origin is

$$\begin{aligned}
\lambda_1 &= \frac{-(\sigma+1) + \sqrt{(\sigma+1)^2 + 4\sigma(r-1)}}{2} \\
\lambda_2 &= \frac{-(\sigma+1) - \sqrt{(\sigma+1)^2 + 4\sigma(r-1)}}{2} < 0 \\
\lambda_3 &= -b < 0.
\end{aligned}$$

The eigenvalues λ_2 and λ_3 are negative for all values of r. The first eigenvalue λ_1 is negative for $0 < r < 1$. We conclude that the origin is a sink (attracting) for $r < 1$ from definition 3.3.2 and theorem 3.4.1.

4.3. Global Stability of the Origin

In fact, if $r < 1$ then all solutions of the Lorenz system approach the origin as $t \to \infty$. We show that the origin is globally stable (see definition 3.4.1) by constructing the Lyapunov function [16],

$$V(x, y, z) = \frac{1}{\sigma}x^2 + y^2 + z^2.$$

The surfaces of constant V are concentric ellipsoids about the origin. We want to show that if we start from any point on the concentric ellipsoids, we keep moving to smaller ellipsoids as $t \to \infty$. However V is a positive function with local minimum at the origin (thus bounded from below by the origin) and so $V(\mathbf{x}(t)) \to 0$, thus $\mathbf{x}(t) \to 0$ as we expect.

$$\begin{aligned}
\frac{1}{2}\dot{V} &= \frac{1}{\sigma}x\dot{x} + y\dot{y} + z\dot{z} \\
&= \left(yx - x^2\right) + \left(yx - y^2 - xyz\right) + \left(zxy - bz^2\right) \\
&= (r+1)xy - x^2 - y^2 - bz^2.
\end{aligned}$$

b is a positive parameter, therefore the last three terms are all negative. But, the sign of xy changes depending on the sign of x and y. However, completing the square gives

$$\frac{1}{2}\dot{V} = -\left[x - \frac{r+1}{2}y\right]^2 - \left[1 - \left(\frac{r+1}{2}\right)^2\right]y^2 - bz^2.$$

From the above, $\dot{V}$ is clearly non positive. But from the theorem, we need to investigate if $\dot{V}$ could be zero. We see that before $\dot{V}$ could be zero, every term on the right side must be zero. The last term could be zero only if $z = 0$ since b is non-negative parameter. The second term is zero only if $y = 0$. This is because, the assumption that $r < 1$ makes what is in the square bracket non zero. Now if $y = 0$ then we will be left with $-x^2$ from the first term, which is also zero if and only if $x = 0$. This means $\dot{V} = 0$ only if $(x, y, z) = (0, 0, 0)$,

but we have already excluded the origin from the beginning of our proof. See theorem 3.4.2. This proves that the origin is globally stable for $r < 1$. The global stability of the origin shows that λ_1 cannot be complex, thus no limit cycles or chaos for $r < 1$. We realise a supercritical pitchfork bifurcation at the origin as r varies through 1. This results in the birth of the two other symmetric fixed points C^+ and C^-.

4.4. Stability of the Symmetric Equilibrium Points

We recall the other equilibrium points $C^{\pm}$:

$$x^* = y^* = \pm\sqrt{b(r-1)}, z^* = r - 1$$

The Jacobian matrix evaluated at these equilibrium points is

$$J_{c^{\pm}} = \begin{bmatrix} -\sigma & \sigma & 0 \\ 1 & -1 & \mp\sqrt{b(r-1)} \\ \pm\sqrt{b(r-1)} & \pm\sqrt{b(r-1)} & -b \end{bmatrix}$$

C^+ and C^- have the same eigenvalues and the characteristic polynomial has the form

$$P_r(\lambda) = \lambda^3 + (b + \sigma + 1)\lambda^2 + b(r + \sigma)\lambda + 2b\sigma(r - 1)$$

The result of computing the eigenvalues is cumbersome and not helping. However, we can extract some information from the characteristics polynomial. Applying the Routh Hurwitz stability criterion discussed in section 3.4.1 to the characteristic polynomial, we obtain the array;

λ^3	1	$b(r+\sigma)$
λ^2	$b+\sigma+1$	$2b\sigma(r-1)$
λ^1	H	0
λ^0	$2b\sigma(r-1)$	0

where

$$H = \frac{b(r+\sigma)(b+\sigma+1) - 2b\sigma(r-1)}{b+\sigma+1}$$

For stability, we expect $H > 0$, thus the system is stable if

$$\frac{b(r+\sigma)(b+\sigma+1) - 2b\sigma(r-1)}{b+\sigma+1} > 0$$

which is the point when

$$r > \frac{\sigma(\sigma+b+3)}{\sigma-b-1}$$

What if $H = 0$? This is possible. In this case, the system experiences the case (see case 2 of section 3.4.1) where

$$b(r+\sigma)(b+\sigma+1) = 2b\sigma(r-1).$$

As discussed earlier, this signals that imaginary roots or roots of the form $(\lambda + p)(\lambda - p)$ are present. This is because the system is symmetric. Making use of the Descartes' theeorem, the characteristic polynomial has either all three roots negative or a negative root

and two complex roots. See theorem 3.4.3. In any case, there is a negative root and no positive root.

Positive	*Negative*	*Imaginary*	*Total*
0	3	0	3
0	1	2	3

Descartes's theorem shows that $P_r(\lambda)$ may have complex roots. For fixed values of $\sigma = 10, b = 8/3$, we study the behaviour of C^+ and C^- as r varies. Numerical simulation shows that for r near 1, the eigenvalues are all real. Plotting the graph of the characteristic polynomial as r increases indicates that for about $r \geq 1.3456$, there is only one real root which implies the existence of pair of complex eigenvalues. The real part of the complex eigenvalues is negative for small $r > 1.3456$. See figure 4.3.
We want to investigate if $P_r(\lambda)$ can have purely imaginary roots. We assume $\lambda = i\omega$ as eigenvalues and substitute $\lambda = i\omega$ in $P_r(\lambda)$ and equating the real and imaginary parts of $P_r(i\omega)$ to zero. Thus;

$$\begin{aligned} -i\omega^3 - \omega^2(\sigma + b + 1) + i\omega b(r + \sigma) + 2b\sigma(r - 1) = 0 \\ i\omega\left(-\omega^2 + b(r + \sigma)\right) - \omega^2(\sigma + b + 1) + 2b\sigma(r - 1) = 0 \end{aligned}$$

Equating the real and imaginary parts to zero, we obtain

$$\begin{aligned} \omega^2 = b(r + \sigma) &= \frac{2b\sigma(r - 1)}{\sigma + b + 1} \\ (r + \sigma)(\sigma + b + 1) &= 2\sigma(r - 1) \\ r_h &= \frac{\sigma(\sigma + b + 3)}{\sigma - b - 1}, \quad \sigma > b + 1 \end{aligned}$$

For $\sigma = 10$ and $b = 8/3$, there is a pair of purely imaginary eigenvalues at $r_h \approx 24.74$ we have that C^+ and C^- are stable in the parameter range $1 < r < 24.74$. For values of r near r_h, there is a "center manifold", a two-dimensional surface, toward which the system attracts. The orbit appears for values of $r < r_h$ and is unstable within the center manifold. The periodic orbit is a saddle in the whole phase space since the real root is negative for all r [13]. At $r = r_h$, the system experiences a subcritical Hopf bifurcation as the equilibrium points lose their stability by absorbing a non-stable periodic orbit [13]. When the complex eigenvalues cross the imaginary axis, the periodic orbit die in Hopf bifurcation at the fixed points C^+ and C^-. When $r > r_h$, the complex roots have positive real part and C^+ and C^- are unstable.

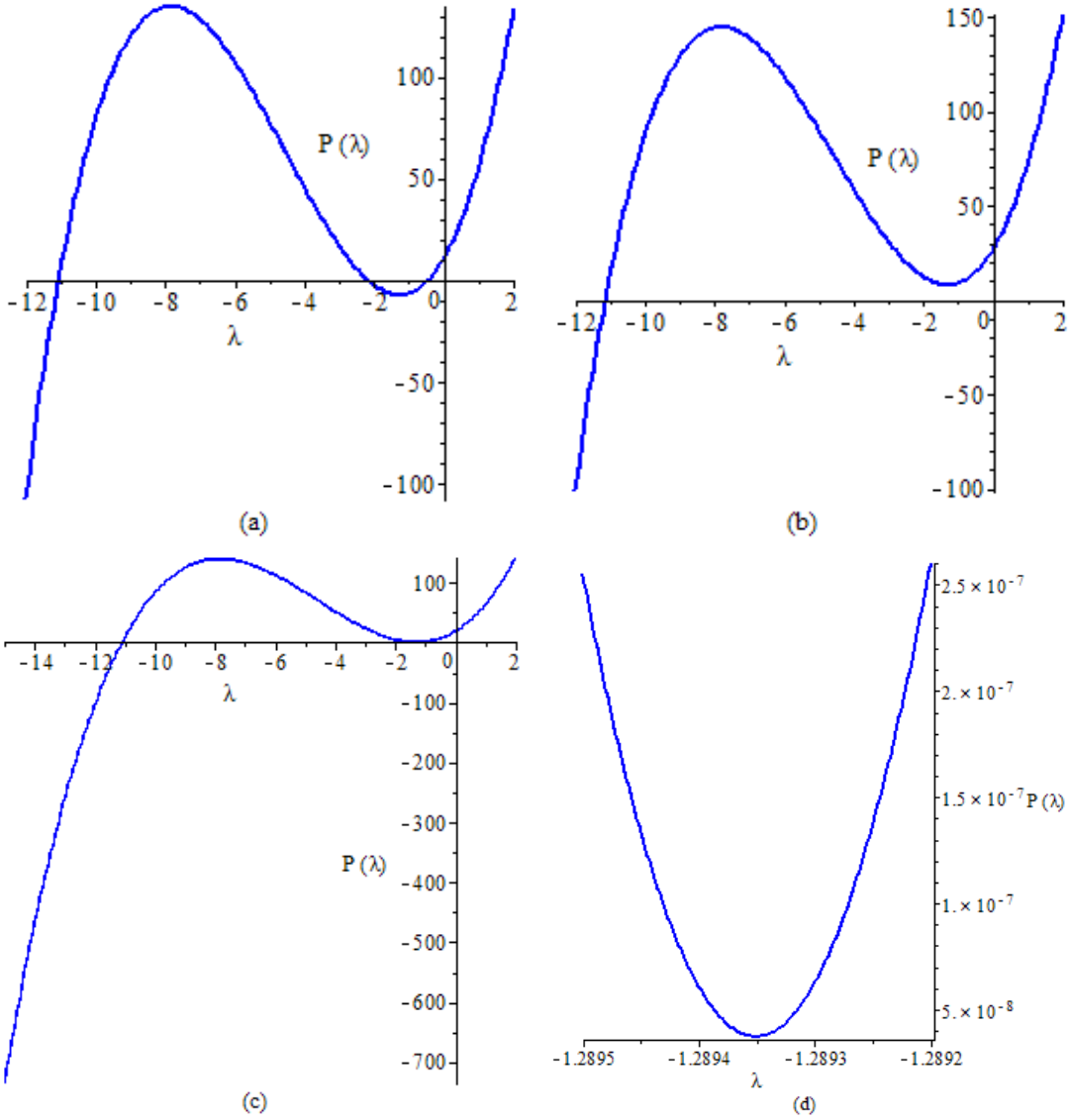

Figure 4.3: Plot of the characteristic polynomial for (a) $r = 1.2$, (b) $r = 1.5$, (c)$r = 1.3456171795$, (d)$r = 1.3456171795$.

4.5. Homoclinic orbits and Bifurcation

In [15], C. Sparrow discusses the homoclinic orbits (see section 3.5) of the Lorenz system. When $r > 1$, the two dimensional stable manifold of the origin (a sheet-like plane) from which the trajectories tend towards the origin divides $\mathbb{R}^3$ into two halves. Trajectories started in one half-space converge to C^+ whereas trajectories started in the other half-space converge to C^-. The stable manifold trajectories of the origin tend towards the origin [15]. For $r' = 13.926$, the spirals formed by the trajectories starting on the unstable manifold of the origin by the positive eigenvalues at the origin grow larger and larger. For $r > r'$, trajectories started on the unstable of the origin will lie in the stable manifold of the origin and will therefore tend, in both forwards and backwards time, towards the origin. Thus, a homoclinic orbit is formed with the stationary point at the origin.[14], proves the existence of homoclinic orbit of the Lorenz system when $r' = 13.926, b = 8/3$ and $\sigma = 10$. We show here by graphs, the existence of homoclinic orbits at the origin of the Lorenz sys-

tem. We take two parameters $13 < 13.926$ and $r = 14 > 13.926$ and study the behaviour of the trajectories starting from the same initial point (0.1, 0.17143, 0.00101) in space and $x - y$ projection respectively. The trajectory starting from the initial point (0.1, 0.17143, 0.00101) tends to C^+(5.6569,5.6569,12) for the parameters $r = 13, \sigma = 10, b = 8/5$. See figure 4.4 for the graph in space and the corresponding $x - z$ projection. The trajectory

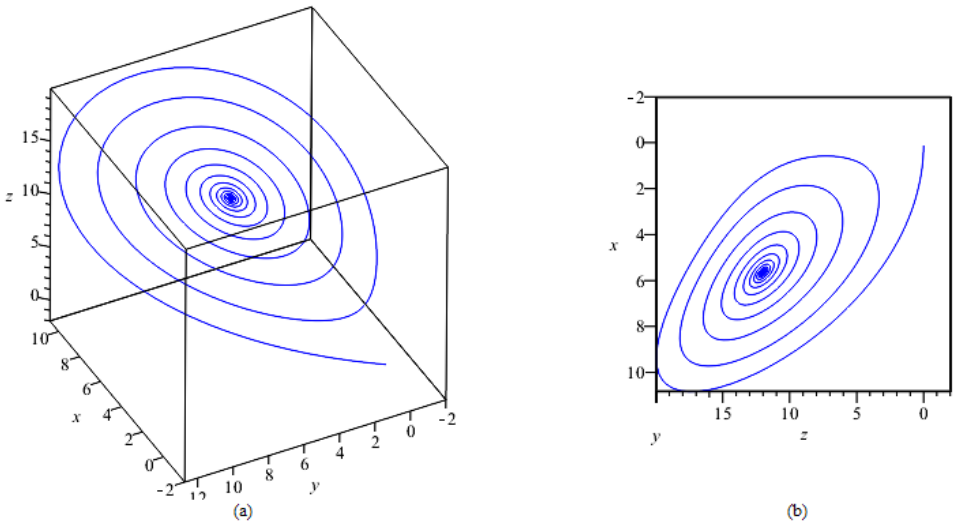

Figure 4.4: Graph of (0.1, 0.17143, 0.00101) converging to $C^+(5.6569, 5.6569, 12)$ (a) in space and (b) corresponding x–z projection for the parameters $r = 13, \sigma = 10, b = 8/3$.

starting from the initial point (0.1, 0.17143, 0.00101) tends to $C^-(-5.8878, -5.6569, 13)$ for the parameters $r = 13, \sigma = 10, b = 8/5$. See figure 4.5 for the graph in space and the corresponding $x-z$ projection. The trajectory starting from the initial point (0.1, 0.17143,

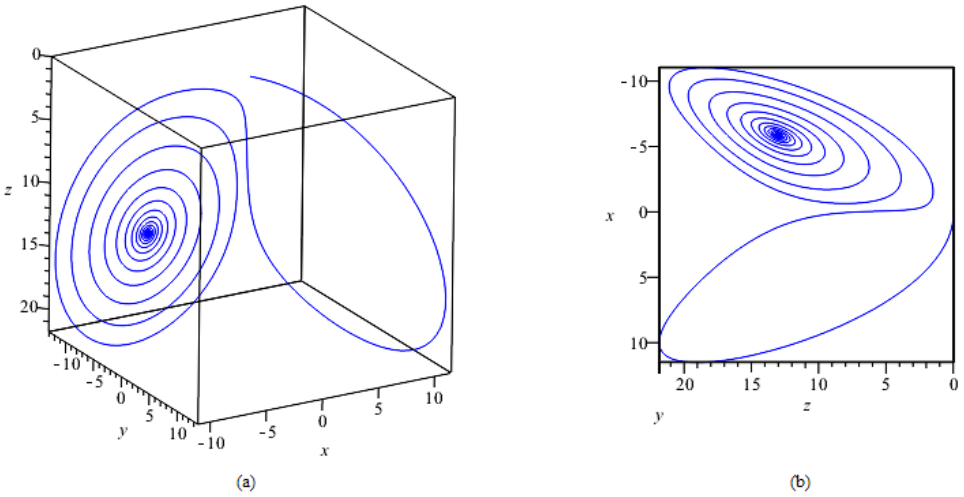

Figure 4.5: Graph of (0.1, 0.17143, 0.00101) converging to $C^-(-5.8878, -5.6569, 13)$ (a) in space and (b) corresponding x–z for the parameters $r = 13, \sigma = 10, b = 8/3$.

0.00101) with the parameters $\sigma = 10, b = 8/3$ forms a homoclinic orbit at the origin at $r' = 13.926$. See figure 4.6 for the graph in space and the corresponding x–z projection. We see the formation of a homoclinic orbit even better as we get closer to the origin. See figure 4.7 for the homoclinic orbit at the origin starting from the initial condition (0, 0.5,

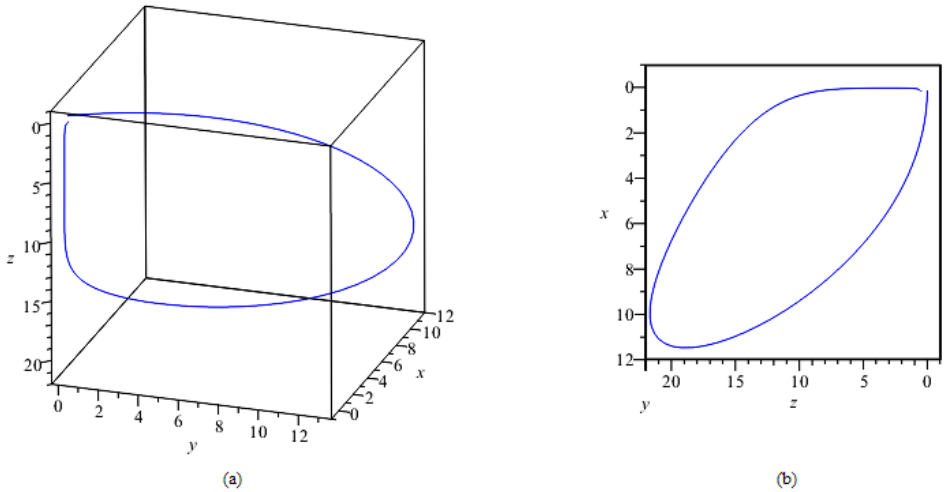

Figure 4.6: Homoclinic orbit formed (a) in space (b) corresponding x – z projection at (0.1, 0.17143, 0.00101) for the parameters.$\sigma = 10, b = 8/3$ and $r' = 13.926$

0) with the parameters $r' = 13.926, \sigma = 10, b = 8/3$ The positive semi-orbit and negative-

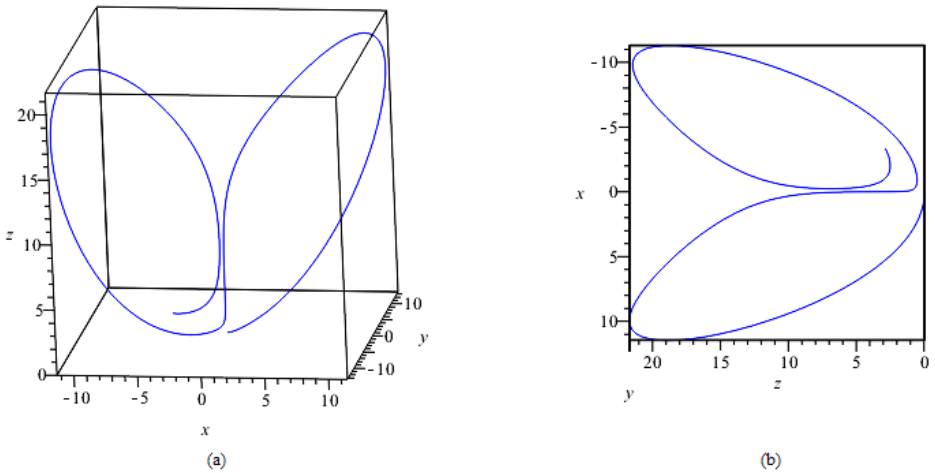

Figure 4.7: Homclinic orbit formed (a) in space (b) corresponding x–z projection at (0,0.5,0) for the parameters $\sigma = 10, b = 8/3$ and $r' = 13.926$.

semi orbit intersect at (0.00306236832762012, - 0.00229328921050086,1.8176). At this point the Lorenz system forms a homoclinic orbit [14].
The table below present a summary of the Lorenz system for different values and range of r.

r value	Bifurcation for the Lorenz system
$1 < r$	The origin is unstable, with two negative eigenvalues and one positive eigenvalue.
$1 < r < r_h$	The equilibrium points $C^{\pm}$ are stable. For$r$ larger than about 1.35, there is one negative real eigenvalue and a pair of complex eigenvalues with negative real parts
$r = r^{'}$	The system experiences a homoclinic bifurcation of periodic orbit which continues up to the subcritical Andronov-Hopf bifurcation at $r = r_h$
$r = r_h$	There is a subcritical Andronov-Hopf bifurcation. The periodic orbit can be continued back to the homoclinic bifurcation at $r = r^{'}$
$r_h < r$	The fixed points $C^{\pm}$ are unstable. There is one negative real eigenvalue and a pair of complex eigenvalues with positive parts.
$r = 28$	A chaotic attractor is observed.

Table 4.1: Bifurcation for the Lorenz system as r-varies.

4.6. Preturbulence

The stationary points C^+ and C^- are stable (attracting) before the r_h - Hopf bifurcation as discussed earlier, so trajectories eventually spirally in toward one of them. However, the trajectories wander close to the stationary point. This phenomena is known as preturbulence. See figure 4.8.

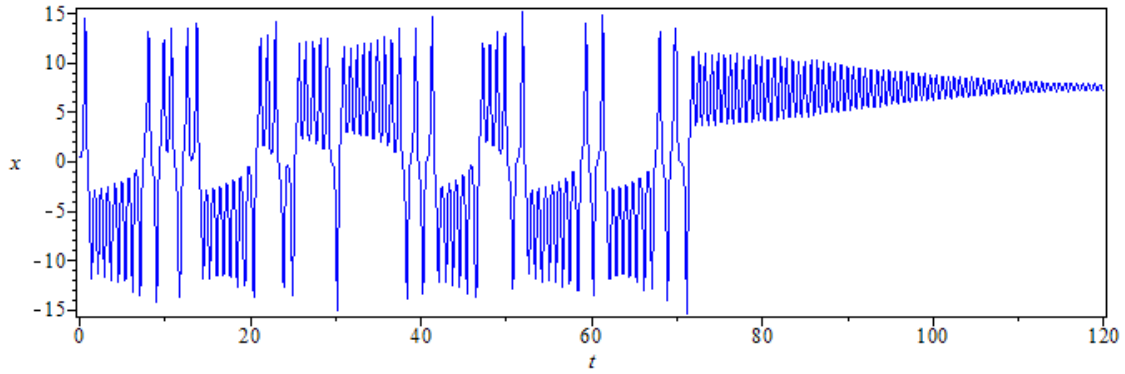

Figure 4.8: preturbulent trajectory at $r = 22.4$ before spiralling into C^+.

According to [15], the average time of wandering by a trajectory which wanders at all, tends to infinity when $r_A \approx 24.06$. Not all trajectories will show preturbulent behaviour in $r < r_A$. Trajectories started near the origin do not show preturbulent behaviour. Also, trajectories started close to the stationary points C^+ and C^- converge to these stationary points without wandering near the strange invariant set [15].

4.7. Chaos on a Strange Attractor

We continue our analysis for $r > r_A$, particularly for the famous parameters $\sigma = 10, b = 8/3, r = 28$ as used by Lorenz. The solutions settle into an irregular oscillation that persists as $t \to \infty$, but never repeats exactly [16]. See figure 4.9. Notice the motion

r value	Description
$0 < r < 1$	The origin is globally stable.
$1 < r$	The origin is non-stable. The flow linearized around the origin has two negative, and one positive, real eigenvalues.
$1 < r < r_h$	The stationary points $C^{\pm}$ are stable.All three eigenvalues of the flow, linearized about C^+ and C^- have negative real part. Providing $r > 1.346$ (σ= 10.b=8/3) there is a complex conjugate pair of eigenvalues.
$r_h < r$	The stationary points $C^{\pm}$ are non-stable. The flow linearized around C^+ and C^-, has one negative real eigenvalue and a complex conjugate pair of eigenvalues with positive real part.
$r > 24.74$	All three stationary points are non-stable.

Table 4.2: Summary of results of the Lorenz system.

is regular for some few time and then jumps into an unending, unpredictable irregular motions. The $x - y$ phase space is shown in figure 4.9 The trajectories do not cross each

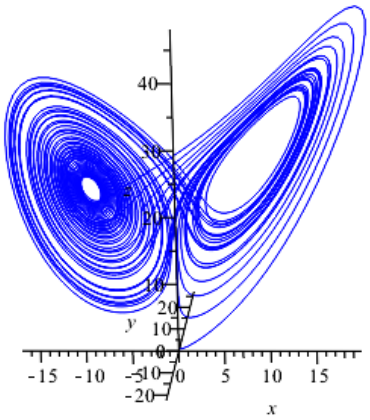

Figure 4.9: x – z phase space at (0, 1, 0) for the Lorenz parameters.

other as they appear. There is no self - intersections occurring in the above figure. The trajectory starts near the origin, then swings to the right and dives into the center of a spiral on the left. It orbits outwards slowly, and then shoots over to spiral around the left loop, jumping forth and back indefinitely. The number of orbiting it makes on either side varies unpredictably from cycle to the next. Table 4.2 presents a summary of the analysis of the Lorenz system. The switching between left and right correspond to the irregular reversals of the waterwheel [16].

4.8. Lorenz Map

Most of the analysis of the Lorenz system has used the Poincaré map. Lorenz wanted to know when the trajectory jumps from the center after a number of spiral. Lorenz's idea is that, looking at successive maximum z_n of the z-coordinate along an orbit, z_n should predict z_{n+1} [16]. By, this he observed that the trajectory leaves one spiral only after exceeding some critical distance from the center. This shows that the Lorenz system has some predictive characteristics. The way to do this is to extract the chaotic solution $z(t)$ after a large number of iterations on the strange attractor. The maxima z_n is further extracted from $z(t)$, and successive pairs of maxima (z_n, z_{n+1}) plotted. See figure 4.10. The function $z_{n+1} = f(z_n)$ is called the **Lorenz map**. According to the map, for a given z_0, we can predict z_1 by $z_1 = f(z_0)$. For such a chaotic and random process,

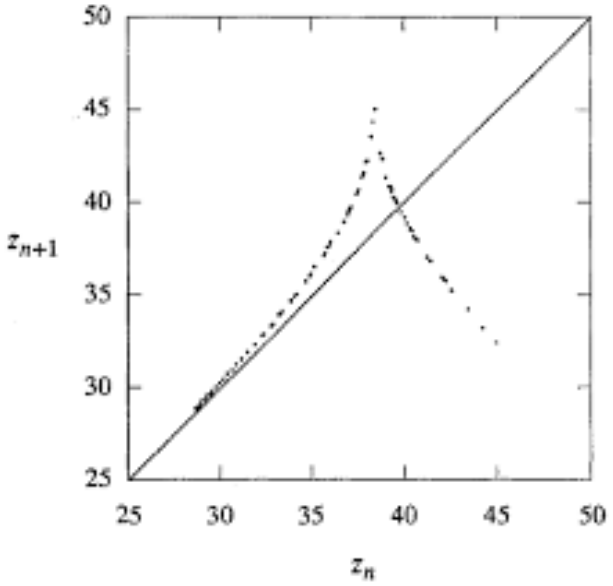

Figure 4.10: The Lorenz map. Source [16].

one may expect a scatter plot. However, the graph shows a quite well-defined relation between successive peaks. Lorenz is right, information about the nth peak gives a good estimate of the next peak, however this is possible for short period. This shows that the solutions of the Lorenz equations have short term predictability. Lorenz discovered some order in the chaos. It also worth mentioning that the Lorenz map is not exactly the Poincaré map we studied in chapter 3, in the sense that, to construct a Poincaré map, for a three-dimensional surface, we compute a trajectory's successive intersections with a two-dimension surface. The Poincaré map takes a point on that surface, specified by *two* coordinates, and then tells us how those two coordinates change after the first return to the surface. In the case of the Lorenz map, the map characterizes the trajectory by only *one* number, not two.

5. Models of the Lorenz Equations

In this chapter we study how the Lorenz equations simulate the chaotic waterwheel as shown by Malkus and Howard at MIT in 1972 and the atmospheric convective model.

5.1. Model for a Waterwheel

The chaotic waterwheel system serves as a mechanical analogue to the Lorenz equation. It was invented by Willem Malkus and Lou Howard at MIT in 1972 to simulate Lorenz equations. We will describe the mechanical model and derive the equations that governs it following [16]. We will then map the waterwheel equations onto Lorenz's equations following [4].

5.1.1. Description of the Waterwheel

The wheel is slightly tilted from the horizontal to allow horizontal rotation of the wheel in both directions (left and right). See figure 5.1.3. Water sprays out through dozens of small nozzles of an overhanging manifold connected to a water pump into separate transparent chambers around the rim of the wheel.
Food colouring is added to the water for easy visibility of the distribution of water around the rim. Each chamber has small hole at the bottom to allow leakage as water fills the champers. The leaked water is collected underneath the wheel, where it is pumped back up through the nozzles to provide a steady input of water.
The system allows for change of parameters in two ways. A brake on the wheel can be adjusted to add more or less friction. The tilt of the wheel can be varied by turning a screw that props the wheel up; this alters the effective strength of gravity [4].
A sensor measures the wheel's angular velocity $\omega(t)$, and sends the data to a strip chart recorder which then plots $\omega(t)$ in real time [4].

5.1.2. The Waterwheel Equations

Now we begin the construction of equations that describes the motion of the waterwheel, to find the mass distribution of water around the wheel's perimeter $m(\theta, t)$ and the angular velocity of the wheel $\omega(t)$. We first identify components contributing to the motion the system.

5.1.3. Conservation of Mass

Water collected underneath the wheel is pumped back into the nozzles to restart the whole process. This means water is conserved. Consider any sector$[\theta_1, \theta_2]$ fixed in space through which the wheel rotates into and out of, as illustrated in the figure 5.2. In this sector, the mass of water changes as a result of rotation of the wheel, the spraying of water into the chambers, and the leakage (outflow) of water out through the hole at the bottom of the chambers.
This can be described mathematically as

$$\frac{dM_{\text{total}}}{dt} = \text{Rotation} + \text{inflow} + \text{outflow} \tag{5.1}$$

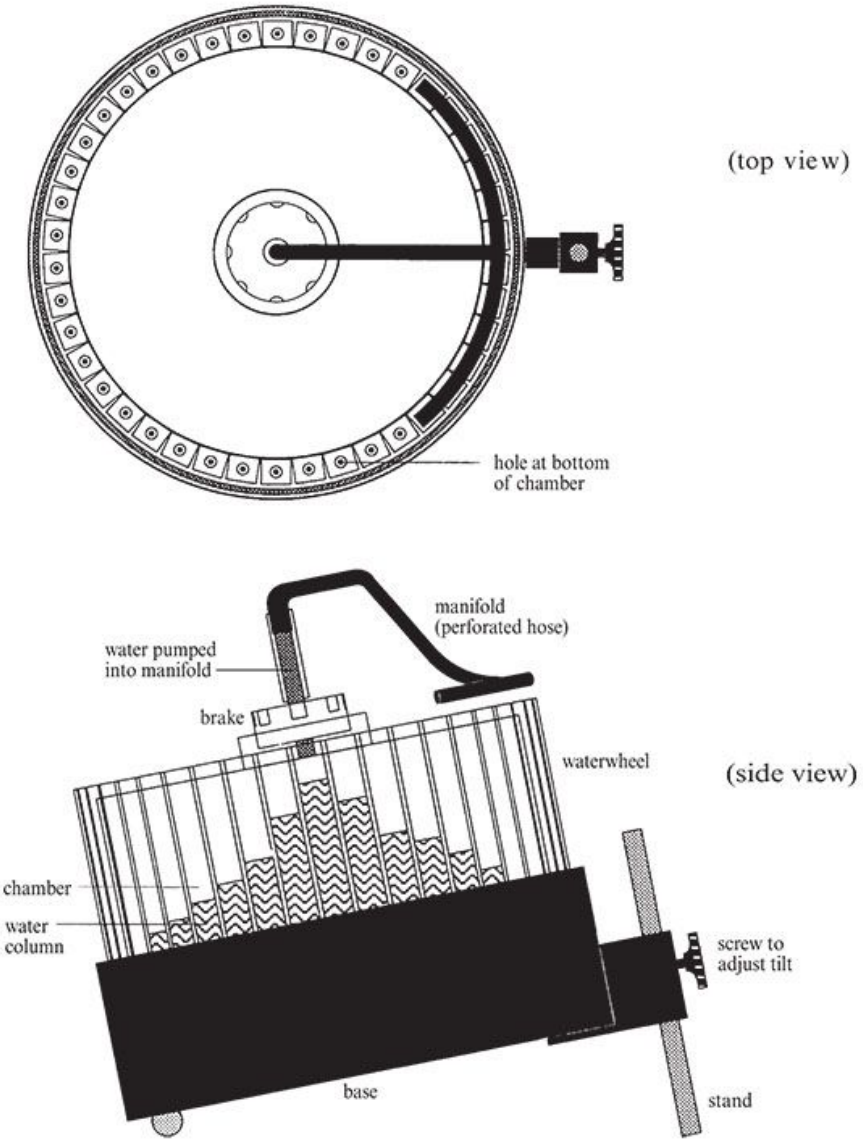

Figure 5.1: The top and side view of the waterwheel, Source [16]

Consider the contribution of the rotation of the wheel. As shown in figure 5.2, let $\omega\Delta t$ be the angle travel in time Δt at start of the sector denoted θ_1. The mass of water at any point in time as it travels toward the other end of the sector marked θ_2 would be $m(\theta_1, t)\omega\Delta t$.
Similarly, the mass of water at any point in time leaving the sector through θ_2 would be obtained as $m(\theta_2, t)\omega\Delta t$. As such, the rate of mass of water resulting from the rotation of water at θ_1 and θ_2 are respectively obtained as $dM_{R1} = m(\theta_1, t)\omega\Delta dt$ and $dM_{R2} = m(\theta_2, t)\omega\Delta dt$ after an infinitesimal time Δt. And so, the total contribution to total mass of water in the sector $[\theta_1, \theta_2]$ due to rotation in the mass change is given as

Symbol	Description	Units ($)
$M_{\text{total}}(t)$	total mass of water in the wheel	kg
$m(\theta, t)$	mass distribution of water around the wheel's perimeter	kg/rad
θ	angle in our lab frame	rad
$\omega(t)$	angular velocity of the wheel	rad/s
Q	water inflow rate	kg/sec
g_0	acceleration due to gravity	m/s^2
R_p	radius of the pipes at the bottom of the syringes	m
l_p	length of the pipes at the bottom of the syringes	m
v_w	viscosity of water	cm^2/s^2
τ	torque on the wheel	$\text{N} \cdot \text{m}$
I	moment of inertia of the wheel	$\text{kg} \cdot \text{m}^2/\text{s}$
α	angle of inclination of the wheel	deg
r^*	radius of the wheel	m
γ	strength of the magnetic brake	$\text{kg} \cdot \text{m}^2/\text{s}$
v	translational velocity of the wheel	m/s
a	translational acceleration of the wheel	m/s^2
a_n, b_n	amplitude coefficients in Fourier series of mass	m
q_n	amplitude coefficients in Fourier series of inflow	kg/s

Table 5.1: Symbols used in model of the wheel. Source [4]

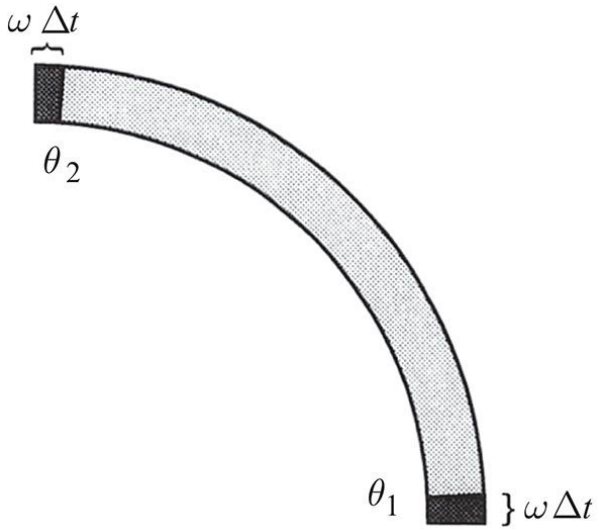

Figure 5.2: Sector view of the waterwheel, Source [16]

$$\frac{dM_{\text{rotation}}}{dt} = \omega(t)\left[m\left(\theta_1, t\right) - m\left(\theta_2, t\right)\right] = -\omega(t)\int_{\theta_1}^{\theta_2} \frac{\partial m(\theta, t)}{\partial \theta} d\theta \tag{5.2}$$

Next we consider the contribution by the outflow. Again as we said in the model description, the hole at the bottom of the chambers allows for a flow (pressure-induced flow) as

water leaks collect underneath the system. The drain or leak is proportional to the mass of water is in the chamber – more water implies a larger pressure, hence faster leakage

$$\frac{dM_{\text{outflow}}}{dt} = -k \int_{\theta_1}^{\theta_2} m(\theta, t) d\theta \tag{5.3}$$

where k is the rate of leakage. We now consider the final component, inflow. Inflow depends on the rate at which water is pumped in through the nozzle. So we have that

$$\frac{dM_{inflow}}{dt} = \int_{\theta_1}^{\theta_2} Q(\theta) d\theta \tag{5.4}$$

The total mass change is therefore obtained by putting all the mass change equations together,

$$\frac{dM_{\text{total}}}{dt} = \int_0^{2\pi} \frac{\partial m}{\partial t} d\theta = \int_0^{2\pi} \left(-\omega \frac{\partial m}{\partial \theta} + Q - km \right) d\theta \tag{5.5}$$

which is same as

$$\frac{\partial m}{\partial t} = Q - km - \omega \frac{\partial m}{\partial \theta} \tag{5.6}$$

Equation (5.6) is called the continuity equation [16].

5.1.4. Torque Balance

Now we will discuss the force causing the motion of the wheel. Torque is the force causing the rotation of the wheel. There are two kinds of torque at play here, thus the damping torque and gravitational torque. Let I be the moment of inertia of the wheel. Then the equation of motion of the wheel is

$$\tau = \text{damping force} + \text{gravitational torque}$$

where g, is the standard acceleration due to gravity, $9.8 m/s^2$. The gravity pull on the chambers is given as

$$\vec{F}_{gravity} = m g_0 \sin \alpha$$

which exerts a torque with magnitude

$$\tau_{gravity} = \vec{r^*} \times \vec{F}_{gravity} = r^* m g_0 \sin \alpha \sin \theta d\theta$$

where r^* is the radius from the wheel's axle to the centre of the chamber. Integration over all mass elements yields

$$\tau_{gravity} = g r^* \int_0^{2\pi} m(\theta, t) \sin \theta d\theta \tag{5.7}$$

where $g = g_0 \sin \alpha$. There are two sources of damping: viscous damping due to the heavy oil in the brake, and damping due to the speeding up of water with zero angular velocity – the water enters the wheel at zero angular velocity but is spun up to angular velocity ω before it leaks out [4]. Both these effects product torques proportional to ω, so we have

$$\text{damping torque} = -v\omega$$

where $v > 0$, with the negative sign implying that the damping opposes the motion. We sum them up to get

$$I\dot{\omega} = -v\omega + gr^* \int_0^{2\pi} m(\theta, t) \sin\theta d\theta. \tag{5.8}$$

So the two equations governing the wheel are

$$\dot{m} = Q - km - \omega \frac{\partial m}{\partial \theta} \tag{5.9}$$

$$I\dot{\omega} = -v\omega + gr^* \int_0^{2\pi} m(\theta, t) \sin\theta d\theta. \tag{5.10}$$

5.1.5. Amplitude Equations

The two equations are not easy to solve and this tells how complicated the motion is. However, we can extract the needed information without having to solve explicitly. The wheel is round and so we can consider the periodicity of mass distribution water in ω. For this reason we can rewrite the equations of the system by Fourier analysis. Since $m(\omega, t)$ is periodic in ω, we we can write it as a sum of various harmonics where a_n and b_n amplitude coefficients for each sine and cosine term respectively:

$$m(\theta, t) = \sum_{n=0}^{\infty} [a_n(t) \sin n\theta + b_n(t) \cos n\theta] \tag{5.11}$$

Similarly, we can write the inflow as a Fourier series:

$$Q(\theta) = \sum_{n=0}^{\infty} q_n \cos n\theta. \tag{5.12}$$

Unlike equation (5.11), equation (5.12) has no $\sin n\theta$ terms in the series. This is because water is added symmetrically at the top of the wheel; the same inflow occurs at θ and $-\theta$ [16]. Now we can substitute the Fourier series equations into equations (5.9) and (5.10) to get a set of ODEs, thus the amplitude equations for the amplitudes a_n, b_n of the different harmonics [16]. We get

$$\begin{aligned} \frac{\partial}{\partial t}\left[\sum_{n=0}^{\infty} a_n(t) \sin n\theta + b_n(t) \cos n\theta\right] = &- \omega \frac{\partial}{\partial \theta}\left[\sum_{n=0}^{\infty} a_n(t) \sin n\theta + b_n(t) \cos n\theta\right] \\ &- K\left[\sum_{n=0}^{\infty} a_n(t) \sin n\theta + b_n(t) \cos n\theta\right] + \sum_{n=0}^{\infty} q_n \cos n\theta. \end{aligned} \tag{5.13}$$

Now we carry out differentiate on both sides, and collect terms. By orthogonality of the functions $\sin n\theta, \cos n\theta$, we can equate the coefficients of each harmonic separately [16]. We get for the sine coefficients,

$$\frac{\partial}{\partial t} a_n = n\omega b_n - k a_n \tag{5.14}$$

Similarly, matching coefficients of gives

$$\frac{\partial}{\partial t}b_n = -n\omega a_n - kb_n + q_n \tag{5.15}$$

In same way, we substitute the Fourier series for the torque. This gives

$$\begin{aligned}\tau_{\text{total}} &= I\dot{\omega} = -v\omega + gr^* \int_0^{2\pi} \left[\sum_{n=0}^{\infty} a_n t \sin n\theta + b_n t \cos n\theta\right] \sin\theta d\theta \\ &= -vw + gr^* \int_0^{2\pi} a_1 \sin^2\theta d\theta \\ &= -v\omega + \pi g r^* a_1.\end{aligned} \tag{5.16}$$

Again by the orthogonality of the sine, cosine functions inside the integral, only one term makes it past the integration [16]. This is the reason why we get only a_1 in the resulting torque equation. We can see from (5.14), (5.15) and (5.16) that a_1, b_1, and ω form a closed system and decouple from all the other a_n and b_n where $n \neq 1$, we can solve the system without them. Therefore ignoring all equations (5.14) and (5.15) where $n \neq 1$, we end up with only three equations

$$\begin{aligned}\dot{a}_1 &= \omega b_1 - ka_1 \\ \dot{b}_1 &= -\omega a_1 - k\dot{b}_1 + q_1 \\ \dot{\omega} &= \tfrac{-v\omega + \pi g r^* a_1}{I}.\end{aligned} \tag{5.17}$$

The system of equations (5.17) is similar to the Lorenz system (4.1). It has two nonlinear components just like the Lorenz system. In the rest of this section, we discuss properties of the waterwheel equations (5.17) and the similarities between the Lorenz system (4.1) and the waterwheel system (5.17).

5.1.6. Fixed Points of the Waterwheel Equations

As usual, we find the fixed points of the system of equations (5.17) by setting all the derivatives equal to zero. This yields;

$$a_1 = \frac{\omega b_1}{k} \tag{5.18}$$

$$a_1 = \frac{q_1 - kb_1}{\omega} \tag{5.19}$$

$$a_1 = \frac{v\omega}{\pi g r^*} \tag{5.20}$$

Equating equations (5.18) and (5.19), we obtain b_1 as

$$b_1 = \frac{q_1 k}{\omega^2 + k^2}. \tag{5.21}$$

Equating (5.17) and (5.19) yields

$$\begin{aligned}\frac{\omega b_1}{k} &= \frac{v\omega}{gr^*\pi} \\ \omega(b_1 gr^* - vk) &= 0,\end{aligned}$$

which implies either $\omega = 0$ or $b_1 = kv/gr^*\pi$. We obtain two kinds of fixed points to consider:

1. $\omega = 0$: if $\omega = 0$, then $a_1 = 0$ and $b_1 = q_1/k$ so we get the fixed point, $(a_1, b_1, \omega) = (0, q_1/k, 0)$. This means the wheel has no angular velocity. Thus the wheel is at rest symmetrically by the water in each chamber. We have the inflow of water balanced by leakage. In the Lorenz system, this is the fixed point at the origin.

2. $\omega \neq 0$: if $\omega \neq 0$, then $b_1 = kq_1/\omega^2 + k^2 = kv/\pi gr^*, k \neq 0$ and

$$\omega^2 = \frac{\pi gr^* q_1}{v} - k^2 \tag{5.22}$$

   There are two possible solutions $\pm\omega$ for equation (5.22), corresponding to a constant angular velocity or steady rotation in either direction. However, the solution exists if and only if

$$\frac{\pi gr^* q_1}{k^2 v} > 1 \tag{5.23}$$

   since angular velocity cannot be imaginary.

The fraction $\pi gr^* q_1/k^2 v$ in (5.23) is the ratio of forcing to the damping of the waterwheel. It is called the Rayleigh number. This is the parameter r in the Lorenz system (4.1). The parameters g and q_1 (gravity and inflow) in the number of the Rayleigh represent the driving of the wheel, whereas the parameters v and k (damping forces and leakage) represent the dissipation of the rotation of the wheel [4]. And so the Rayleigh number gives a measure of how much the damping forces and leakage/outflow is dissipating the driving force of the waterwheel.
In (5.23), $\pi gr^* q_1 > k^2 v$ implies that a steady motion is possible only if the driving force is large enough to overcome the dissipation (stopping force) [4]. The applications of the Rayleigh number is much prevalent in fluid problem. This was obtained by Lord Rayleigh when he studied the problem of a thin layer of fluid heated from below or cooled from above. He achieved a straightforward criterion, the Rayleigh number is proportional to the temperature difference from bottom to top. No convective motion is observed at low values of the Rayleigh number, the fluid transports heat exclusively by molecular heat diffusion. However, at Rayleigh number slightly exceeding a critical value, an instability occurs. Fluid at the bottom (close to the heat source) get hot and less dense and start to rise to the top while the cold heavy fluid on top begins to sink simultaneously. The pattern becomes unstable and the convection eventually becomes chaotic as the Rayleigh number is several times the critical value.
This is not only comparable to the atmospheric convections (where air close to the earth surface get less dense and rise to the top forming clouds above while cold air sinks closer to the earth) but also to the steady rotation of our waterwheel. At higher Rayleigh number, the system becomes turbulent, and the convective motion becomes complex in space and breaks the analogy to our waterwheel. At this point the convection roll remains chaotic while the waterwheel settles into a pendulum-like pattern of reversals, turning once to the left, then back to the right, and so on indefinitely. We can achieve this contrast in our waterwheel by setting the angle of inclination high with a low breaking force.

5.1.7. Relating the Waterwheel Equations to the Lorenz Equations

We are ready to map or relate the two systems of equations. Recall the Lorenz's equations:

$$\dot{x} = \sigma(y - x) \tag{5.24}$$

$$\dot{y} = rx - y - xz \tag{5.25}$$

$$\dot{z} = xy - bz \tag{5.26}$$

and the waterwheel equations;

$$\begin{aligned} \dot{a}_1 &= \omega b_1 - k a_1 \\ \dot{b}_1 &= -\omega a_1 - k b_1 + q_1 \\ \dot{\omega} &= \tfrac{-v\omega + \pi g r^* a_1}{I}. \end{aligned}$$

By examining the position of the variables of the Lorenz equations and the waterwheel equations, we can match the two system of equations as follows

$$\dot{\omega} = \frac{g r^* a_1 \pi - v\omega}{I} \quad \Leftrightarrow \dot{x} = \sigma(y - x) \tag{5.27}$$

$$\dot{a_1} = \omega b_1 - k a_1 \quad \Leftrightarrow \dot{y} = rx - y - xz \tag{5.28}$$

$$\dot{b}_1 = -\omega a_1 - k b_1 + q_1 \Leftrightarrow \dot{z} = xy - bz \tag{5.29}$$

The Lorenz equations are dimensionless [4]. The waterwheel equations are dimensional and so the first thing we need to do is to transform the waterwheel equations into a dimensionless form. We will achieve this by a simple change of variables of the waterwheel equations which sets them to a dimensionless form and then match the corresponding variables of the two sets of equations.

5.1.8. Change of Variables

We create a relation between corresponding variables of the equivalent equations. For instance to obtain the Lorenz variable x from the waterwheel variable ω (we already said these two variables are equivalent), we divide ω by some constant γ (which is same unit as ω) in order to make this term dimensionless (since the units cancel out).

$$x = \frac{\omega}{\gamma}$$

We add x_0 as an offset

$$x = x_0 + \frac{\omega}{\gamma}$$

$$\omega = \gamma(x - x_0)$$

Similarly

$$y = y_0 + a_1/\alpha \Rightarrow a_1 = \alpha\,(y - y_0)$$

$$z = z_0 + b_1/b \Rightarrow b_1 = b\,(z - z_0)$$

and also a dimensionless time

$$T = \frac{t}{\tau} \Rightarrow t = T\tau$$

where γ,α,b and T are constants. ω,b_1 and a_1 are variables of the waterwheel equations. So we have from equation (5.27)

$$\frac{d\omega}{dt} = \dot{\omega} = \frac{\partial\gamma\,(x - x_0)}{\partial T\tau} = \frac{\gamma}{T}\frac{dx}{d\tau} = \frac{\gamma}{T}\dot{x} \Rightarrow \dot{x} = \frac{T}{\gamma}\dot{\omega} \tag{5.30}$$

Therefore we can write that

$$\sigma(y - x) = \frac{T}{\gamma}\left(\frac{gr^*a_1\pi - v\omega}{I}\right).$$

Substituting for $a_1 = \alpha(y - y_0)$

$$\sigma(y - x) = \frac{T}{I\gamma}\left(gr^*\pi\alpha\,(y - y_0) - v\gamma\,(x - x_0)\right)$$

we simplify the terms on the right in order to match terms

$$\sigma(y - x) = \frac{T}{I\gamma}\left(-v\gamma x + v\gamma x_0 + \pi gr^*\alpha y - \pi gr^*\alpha y_0\right)$$

we obtain the following by matching the terms

$$\frac{T}{I}v = \sigma \tag{5.31}$$

$$\frac{T}{I\gamma}\pi gr^*\alpha = \sigma \Rightarrow \alpha = \frac{v\gamma}{\pi gr^*} \tag{5.32}$$

Likewise, from equation (5.28)

$$\frac{da_1}{dt} = \dot{a}_1 = \frac{\partial\alpha\,(y - y_0)}{\partial T\tau} = \frac{\alpha}{T}\frac{dy}{d\tau} = \frac{\alpha}{T}\dot{y} \Rightarrow \dot{y} = \frac{T}{\alpha}\dot{a}_1$$

we can write that

$$rx - y - xz = \frac{T}{\alpha}\left(\omega b_1 - ka_1\right)$$

substituting for $\omega = \gamma(x - x_0), a_1 = \alpha(y - y_0), b_1 = b(z - z_0)$

$$rx - y - xz = \frac{T}{\alpha}\left(\gamma bxz - \gamma bz_0x - \gamma bx_0z + \gamma bx_0z_0 - k\alpha y + k\alpha y_0\right)$$

Matching components yields

$$Tk = 1 \tag{5.33}$$

$$\frac{T}{\alpha}\gamma b = -1 \tag{5.34}$$

$$-\frac{T}{\alpha}\gamma bz_0 = r \tag{5.35}$$

$$\frac{\tau}{\alpha}\left(-\gamma bx_0z + \gamma bx_0z_0 + k\alpha y_0\right) = 0 \tag{5.36}$$

Equation (5.34) combined with equation (5.35) gives $z_0 = r$. In the last equation, $z_0 \neq 0, k \neq 0, \alpha \neq 0, \gamma \neq 0$ implies that $x_0 = y_0 = 0$. Finally, we get for the last relation

$$\frac{db_1}{dt} = \dot{b}_1 = \frac{\partial b\,(z - z_0)}{\partial T\tau} = \frac{\alpha}{T}\frac{dz}{d\tau} = \frac{\alpha}{T}\dot{z} \Rightarrow \dot{z} = \frac{T}{b}\dot{b}$$

We can write that

$$xy - bz = \frac{T}{b}\left(-\omega a_1 - kb_1 + q_1\right)$$

Again we substitute to obtain

$$xy - bz = \frac{T}{b}\left(-\gamma\alpha xy + \gamma\alpha xy_0 + \gamma\alpha x_0 y - \gamma\alpha x_0 y_0 + kb - kbz + kbz_0 + q_1\right)$$

$$T\gamma\alpha = -1 \tag{5.37}$$

$$Tk = b \tag{5.38}$$

$$\frac{T}{b}\left(\gamma\alpha y_0 x + \gamma\alpha y x_0 - \gamma\alpha y_0 x_0 + kbz_0 + q_1\right) = 0 \tag{5.39}$$

Equation (5.37) with equation (5.34) yields $\alpha = \pm b$. Also equation (5.38) with equation (5.33) implies $Tk = b = 1$. Substituting $x_0 = y_0 = 0$ into equation (5.39), we end up with

$$kbz_0 + q_1 = 0 \Rightarrow z_0 = -\frac{q_1}{bk} \tag{5.40}$$

Finally, equation (5.37) and equation (5.38) with $\alpha = -b$ gives $\gamma = k$. And so the waterwheel is equivalent to the Lorenz equation if

$$a_1 = \alpha y = \frac{v\gamma}{\pi g r} y = \frac{kv}{\pi g r} y$$

$$b_1 = \frac{-kv}{\pi g r} z + \frac{q_1}{k}$$

$$\omega = kx$$

$$T = \frac{1}{k}$$

$$\sigma = \frac{v}{kI}$$

and the Rayleigh number

$$r = \frac{\pi g r^* q_1}{k^2 v}.$$

Also, $Tk = b = 1$ tells us the waterwheel is a specific case of the Lorenz equations. The waterwheel equation translates into the Lorenz equation when the Lorenz parameter $b = 1$.

5.2. Atmospheric Convective Model

In 1963, Lorenz in his attempt to predict the weather with a much easier-to-analyse model than partial differential equations discovered the system of equations (4.1), named after E. N. Lorenz. The Lorenz system also describes the convection rolls in the atmosphere. That is, air particles close to the earth get heated up and becomes less dense and as a result, rises up into the atmosphere where it gets cooled. The uprising of less dense air particles are replaced by a relatively dense layer of air particles closer to the earth. The process continues, forming what is called convective rolls.
In Lorenz's work, he considered a two-dimensional fluid cell that was heated from below and cooled from above. The heating causes changes in the temperature of the fluid. This change corresponds to the varying of the control parameter, Rayleigh number in our analysis. The difference in temperature plays a role similar to the difference of the rate of adding water for the waterwheel . The chaotic orbits correspond to the atmosphere forming a convective roll in one direction for a length of time and then reversing and rolling in the other direction. The number of rolls in each direction before the reversal is apparently random [13].
He simplified the infinitely many variables involved into the three dimensional system of equations (4.1). The independent variable is the rate of convective "overturning", y and z measures the horizontal and the vertical temperature variation respectively . The system parameters are; the Prandtl number σ, the Rayleigh number r, and b that is related to the physical size of the system [13].

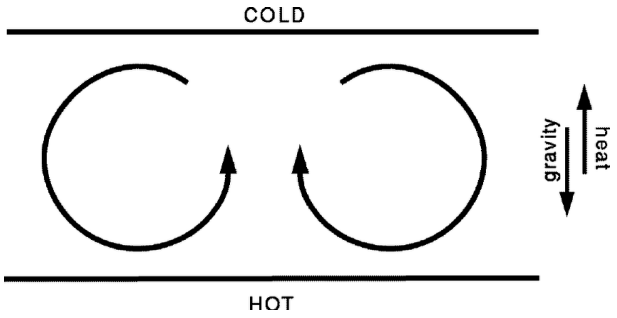

Figure 5.3: Convection rolls for fluid.

6. Conclusion

In conclusion, the goals of the thesis as proposed earlier have been achieved. Important concepts of the field of dynamics such as equilibrium points, stability, linearization, bifurcation, Lyapunov function, Poincaré map, strange attractors and chaos are studied. Also, a description of how the Lorenz equations arise in various models are studied. However, it is worth noting that this is just a tip of the iceberg. There is still much to study about the Lorenz equations.

In view of this, we recommend that furhter study of the subject include Tent map, Warwick Tucker's computer assisted proof, geomeotric model of the Lorenz equations as introduced by Guckenheimer and the Lyapunov exponent as a tool to measure chaos. We also propose further studies for r beyond the value of 28.

Another interesting topic for study is to consider the variation of the other parameters σ, b and not just r.

Bibliography

[1] ANDERSON, K. G.,*Poincare's discovery of homoclinic points*, Arch.Hist Exact. 1994, Sci., Vol.48 (1994), 133-147.

[2] BARROW-GREEN, J.*Oscar II's Prize Competition and the Error in Poincare's Memoir on the Three body Problem.* Arch. Hist. Exact. Sci., 48 (1994), 107-131.

[3] DORF, Richard C. and Robert H. BISHOP. *Modern control systems.*12th ed. Upper Saddle River: Prentice Hall, c2011. ISBN 978-0-13-602458.

[4] FORDYCE, Rachel Frost.*Chaotic Waterwheel.* Reed University, 2009, (Vol. 77). Also available from: https://www.reed.edu/physics/faculty/illing/campus/pdf/RachelThesis09.pdf.

[5] GLEICK, James.*Chaos Making a New Science.* USA: Viking Penguin, 1987. ISBN 0-670-81178-5.

[6] HAKEN, H.*Analogy between higher instabilities in fluids and lasers.* Elsevier BV, 1975„ Pages 77-78. Also available from: https://doi.org/10.1016/0375-9601(75)90353-9.

[7] HIRSCH, Morris W., Stephen SMALE and Robert L. DEVANEY.*Differential Equations, Dynamical Systems, and An Introduction to Chaos.* Second Edition. USA: Elsevier, 2004. ISBN 978-0-12-349703-1.

[8] KNOBLOCH, E.*Chaos in the segmented disc dynamo.*Elsevier: Physics Letters A, 2002, 1981 (Vol. 82), Pages 439-440. Also available from: https://doi.org/10.1016/0375-9601(81)90274-7.

[9] KRISHNASWAMI, Govind Sudarshan and Himalaya SENAPATI.*An Introduction to the Classical Three-Body Problem: From Periodic Solutions to Instabilities and Chaos.*2019, (24 (1) .DIO: 10.1007 / s12045-019-0760-1.

[10] MALKUS, W.V.R *Non-periodic convection at high and low Prandtl number.*Mem. Soc. R. Sci. Liege, 1972, (IV (6), 125–128.

[11] MUSIELAK, ZE and B. QUARLES.*The three-body problem.* Cornell University: arXiv.org, 2015, (Vol. 77). DOI: 10.1088 / 0034-4885 / 77/6/065901.

[12] PERKO, Lawrence.*Differential Equations and Dynamical Systems.*Third Edition. USA: Springer-Verlag, New York, 2001. ISBN 0-387-95116-4.

[13] ROBINSON, R. Clark.*An Introduction to Dynamical Systems* . Second Edition. USA: American Mathematical Society, 2012. ISBN 978-0-8218-9135-3.

[14] SONG, Juan, Yanmin NIU and Xiong LI.*The existence of homoclinic orbits in the Lorenz system via the undetermined coefficient method.* Elsevier, 2019„ Pages 497-515. DOI: https://doi.org/10.1016/j.amc.2019.03.011.

[15] SPARROW, Colin. *The Lorenz Equations: Bifurcations, Chaos, and Strange Attractors The Lorenz Equations: Bifurcations, Chaos, and Strange Attractors.*USA: Springer-Verlag New York, 1982. ISBN 978-0-12-349703-1.

[16] STROGATZ, Steven H. *Nonlinear Dynamics and Chaos: With Applications to Physics, Biology, Chemistry, and Engineering.*Second Edition. USA: Westview Press, 2015. ISBN 978-0-8133-4910-7.

[17] TONGEN, A., RJ THELWELL and D. BECERRA-ALONSO. *Reinventing the Wheel: The Chaotic Sandwheel* . American Journal of Physics, 2013, 81 (2), 127-133.

[18] WANG, Xiaoshen. *A Simple Proof of Descartes's Rule of Signs.*The American Mathematical Monthly, 2004, (111(6). DOI: 10.2307/4145072.